

Comparison of Cylindrical Boundary Pasting Methods

by

Shalini Aggarwal

A thesis

presented to the University of Waterloo

in fulfilment of the

thesis requirement for the degree of

Master of Mathematics

in

Computer Science

Waterloo, Ontario, Canada, 2004

©Shalini Aggarwal 2004

I hereby declare that I am the sole author of this thesis. This is a true copy of the thesis, including any required final revisions, as excepted by my examiners.

I understand that my thesis may be made electronically available to the public.

Abstract

Surface pasting is an interactive hierarchical modelling technique used to construct surfaces with varying levels of local detail. The concept is similar to that of the physical process of modelling with clay, where features are placed on to a base surface and attached by a smooth join obtained by adjusting the feature. Cylindrical surface pasting extends this modelling paradigm by allowing for two base surfaces to be joined smoothly via a blending cylinder, as in attaching a clay head to the body using a neck.

Unfortunately, computer-based pasting involves approximations that can cause cracks to appear in the composite surface. In particular this occurs when the pasted feature boundary does not lie exactly over the user-specified pasting region on the base surface. Determining pasted locations for the feature boundary control points that give a close to exact join is non-trivial, especially in the case of cylinders as their control points can not be defined to lie on their closed curve boundary. I propose and compare six simple methods for positioning a feature cylinder's control points such that the join boundary discontinuities are minimized. The methods considered are all algorithmically simple alternatives having low computational costs. While the results demonstrate an order of magnitude quality improvement for some methods on a convex-only curved base, as the complexity of the base surface increases, all the methods show similar performance. Although unexpected, it turns out that a simple mapping of the control points directly onto the pasting closed curve given on the base surface offers a reasonable cylindrical boundary pasting technique.

Acknowledgements

I would like to thank my supervisor, Stephen Mann, for his support, encouragement and guidance throughout my Masters. His knowledge and experience, balanced by patience and compassion, have made him a valued supervisor as well as a trusted friend. Further, I would like to thank my readers, William Cowan and Sanjeev Bedi, who took the time to read and critique my thesis, offering helpful suggestions for improving it.

I am indebted to a special friend and mentor, Wendy Hatch, without whose support I would have been lost. Her unfaltering belief in me gave me the courage to accept, the strength to believe, and the wisdom to move forward despite the antics of a chronic illness. I am infinitely grateful to my family for walking this difficult journey with me, providing unconditional love and caring in every way possible. The analogy of the bumblebee defying all odds to fly, provided by my father, was a great source of inspiration and encouragement. I also sincerely appreciate the much needed technical help and advice I received from the CGL family. Finally, I am thankful to the many friends who have offered shoulders to lean on, cheered me up, and made my years at the University of Waterloo positively memorable.

Financial support for the research in this thesis was provided by NSERC, CITO, and the University of Waterloo.

“Illness is the night-side of life, a more onerous citizenship”¹. I dedicate this work to those who must learn to journey forth with this citizenship, learning from the adversities to discover life more wholistically while continuing towards their dreams from new directions. I hope this thesis will inspire hope and determination to overcome what seems impossible.

¹Susan Sontag in *Illness as Metaphor*

Trademarks

Houdini is a trademark of Side Effects Software.

All other products mentioned in this thesis are trademarks of their respective companies.

Contents

1	Introduction	1
2	Background	3
2.1	B-splines	3
2.1.1	Knot Insertion	5
2.1.2	Knot Multiplicity	6
2.1.3	Curve Evaluation	6
2.1.4	Continuity	7
2.1.5	Closed Curves	7
2.2	Tensor Product Surfaces	9
2.2.1	Tensor Product Cylinders	10
2.3	Surface Pasting	10
2.3.1	Diffuse Coordinate Space	12
2.3.2	Greville Displacement	12
2.3.3	Standard Pasting	13
2.3.4	Cylindrical Pasting	17
3	Towards Improving Cylindrical Pasting	20
3.1	Motivation and Goals	20
3.2	Basics	22
3.3	Greville Paste	23

3.4	Control Point Paste	25
3.5	Directional Displacement Paste	28
3.6	Relative Displacement Paste	31
3.7	Computational Analysis	33
3.8	Error Bounds	35
4	Results	39
5	Conclusions	50
5.1	Summary	50
5.2	Future Work	52
A	Polynomial Paste Curves	53
	Bibliography	57

List of Tables

3.1	Costs of pasting a $m \times 3$ cylinder onto a bicubic patch	35
4.1	Pasting onto a Circular Paste Curve on a Planar Base	41
4.2	Pasting onto a Polynomial Paste Curve on a Planar Base	43
4.3	Pasting onto a Convex Base	45
4.4	Pasting onto a Convex-Concave Base	47
4.5	Another Paste onto a Convex-Concave Base	49
A.1	Pasting onto a Polynomial Paste Curve on a Convex Base	55
A.2	Pasting onto a Polynomial Paste Curve on a Convex-Concave Base	56

List of Figures

2.1	Cubic B-spline	4
2.2	Knot Insertion	5
2.3	Curve Continuity	8
2.4	Bicubic Tensor Product Patch	10
2.5	Bicubic Tensor Product Cylinder	11
2.6	Standard Surface Pasting	14
2.7	Cylindrical Pasting	18
3.1	Zero Greville Displacement Approximations	21
3.2	Greville Paste	24
3.3	Control Point Paste	27
3.4	Directional Displacement Paste	29
3.5	Relative Displacement Paste	32
4.1	Pasting onto a Planar Base	42
4.2	Pasting onto a Convex Base	46
4.3	Pasting onto a Convex-Concave Base	48

Chapter 1

Introduction

Constructing smooth surfaces with multiple levels of control and adjustability that can be modified or animated at interactive rates remains an area open for further research. Hierarchical modelling offers a conceptual basis for generating surfaces with varying levels of detail, thereby encouraging interactive editing at any level. A hierarchical model of a human-like character may start with a torso at the base level, progressively building up to include all body parts such as the limbs and further the fingers or toes. The design suggests that a movement to the character's torso will translate to the rest of the body parts, while finger motion can be local. Rather than having to recompute the entire character for display, this hierarchical structure enables recomputations to be performed only on the affected components making it suitable for computer animation. An additional advantage is that each level of detail becomes reusable for other models.

Several hierarchical modelling techniques exist including hierarchical B-splines [8], displacement mapping [7], and surface pasting [1]. In this thesis I choose to work further with surface pasting due to its advantages over the other known methods, i.e., lower computational costs, lower storage requirements, easy repositioning, and flexibility of non-parametric alignments. Surface pasting was developed by Barghiel, Bartels and Forsey to mimic the physical process of modelling with clay. It allows local detail to be added to a tensor product B-spline surface called the base, by pasting a second tensor product surface, the feature, on to it in a manner that does

not increase the overall complexity of the original surfaces. A tensor product B-spline surface is represented as a set of *control points*. The pasting process involves mapping the feature control points onto the base; in particular, the feature's boundary control points are placed directly on the base in an attempt to create a gap-free join. Features may be pasted hierarchically and may be scaled or moved arbitrarily over their base surfaces, yet the composite surface can be evaluated using relatively low computational resources. These properties facilitate interactive prototyping and previewing of computer-generated surface models, making surface pasting highly suitable for integration into modelling software. However, because surface pasting is an approximation technique, the resulting surfaces often have unacceptably large discontinuities at the feature-to-base joins. The costs associated with traditional refinement using knot insertion are typically too high to allow interactive modelling. Promising alternatives for improving the surface quality while retaining the overall benefits of pasting have been given by applying approximation methods such as quasi-interpolation or least-squares fittings when determining the paste.

Recognizing the value of surface pasting, Mann and Yeung extended the scope of pasting to model surfaces that include tensor product cylinders, calling it cylindrical surface pasting [12]. Joining the previous character's head to its shoulders using a cylindrical neck instead of a patch allows for significantly improved shape control and a more clay-like equivalence. To paste the boundary of a feature cylinder onto the surface of a base the approximations used in standard pasting are directly applied to the feature control points. However, a fundamental construction difference between the closed curve boundary of a tensor product cylinder and the linear boundary of a tensor product patch leads us to believe that this direct application is likely to be inappropriate. In this thesis, I propose and examine five alternative simple and low-cost cylindrical pasting techniques that attempt to account for the feature cylinder's structural difference. Although my new methods appear to offer an order of magnitude improvement in the paste quality of a cylinder on a simple base surface, as the complexity of the base increases the improvement becomes almost insignificant. It turns out that applying the original surface pasting technique to cylindrical pasting is in general as good as any of my methods, a result that was intuitively unexpected.

Chapter 2

Background

The geometric modelling of complex curves and surfaces is typically achieved using polynomial representations such as Bézier and B-spline curves. B-splines are preferred due to their flexibility, compact representation, and adjustable levels of internal continuity. The surface pasting modelling technique we are concerned with in this thesis uses tensor product B-spline surfaces as its building blocks. This chapter begins with an overview of B-splines, drawing upon it to explain concepts relevant to surface pasting. A summary of existing standard and cylindrical pasting techniques follow, forming the ground work for this thesis.

2.1 B-splines

This section establishes basic notation while introducing terms, relations, and details used throughout the rest of this thesis. A more thorough discussion on the material presented here is provided by Farin [6].

A degree m B-spline curve $C(u)$ with L polynomial segments, is mathematically represented as the sum of its control points $\{P_i\}_{i=0}^{L+m-1}$ weighted by their corresponding basis functions $\{N_i^m\}_{i=0}^{L+m-1}$, i.e.,

$$C(u) = \sum_{i=0}^{L+m-1} P_i N_i^m(u).$$

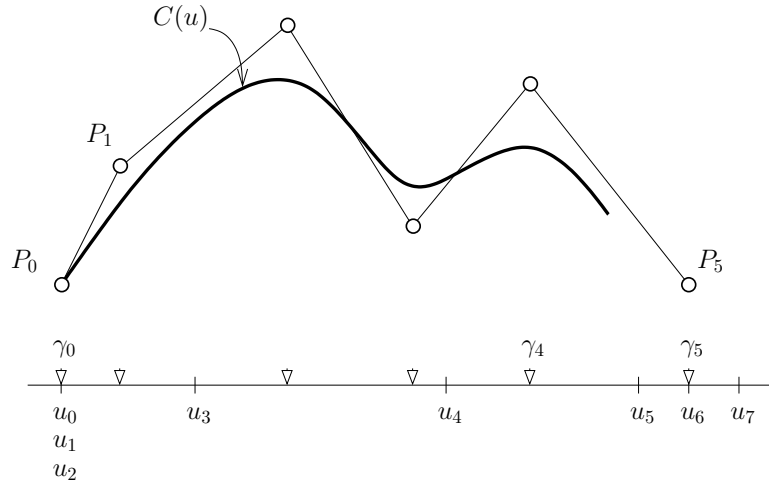


Figure 2.1: A Cubic B-spline with $L = 3$

$C(u)$ is defined over a sequence of non-decreasing domain values known as the knot sequence u_0, \dots, u_{L+2m-2} , with at most m consecutive knots coinciding (Figure 2.1). The basis functions are accordingly determined as the set of $L + m$ linearly independent piecewise polynomials over the linear function space given by the special knot interval $[u_{m-1}, u_{L+m-1}]$. To compute these degree m basis functions a numerically stable recurrence relation is available; the two extra end knots required, u_{-1} and u_{L+2m-1} , may be assigned any arbitrary value as they do not influence the result:

$$N_i^0(u) = \begin{cases} 1 & \text{if } u_{i-1} \leq u < u_i \\ 0 & \text{otherwise} \end{cases}$$

$$N_i^m(u) = \frac{u - u_{i-1}}{u_{i+m-1} - u_{i-1}} N_i^{m-1}(u) + \frac{u_{i+m} - u}{u_{i+m} - u_i} N_{i+1}^{m-1}(u).$$

Each $N_i^m(u)$ is non-zero over $[u_{i-1}, u_{i+m}]$, and attains its maximum when evaluated at $\gamma_i = \frac{1}{m}(u_i + u_{i+1} + \dots + u_{i+m-1})$ for $i = 0, \dots, L + m - 1$. The value γ_i , is called the i th Greville abscissa of C , and is such that P_i maximally influences the curve at $C(\gamma_i)$.

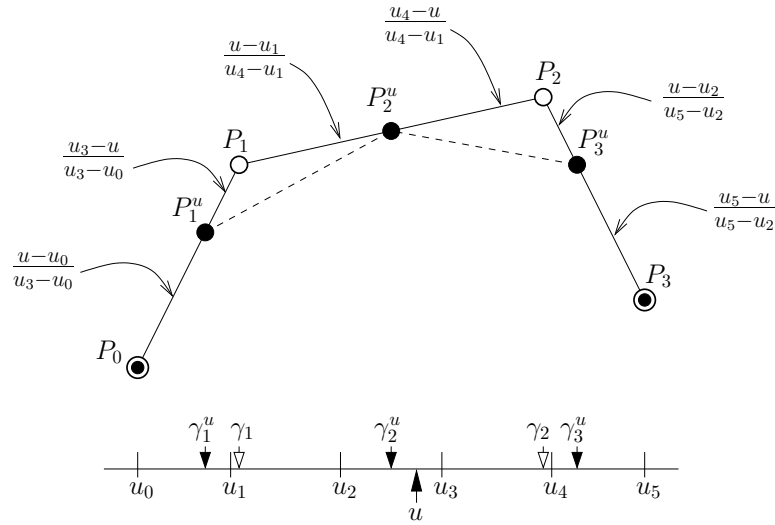


Figure 2.2: Knot Insertion into a Cubic B-spline Polygon – the new knot is u

2.1.1 Knot Insertion

In general, knot insertion is a basic polygon manipulation technique producing one piecewise linear function from another. Applying it to a B-spline polygon facilitates curve refinement.

To understand knot insertion in the context of B-splines, we begin with a degree m B-spline curve having a maximum of L polynomial segments and defined over a non-decreasing knot sequence u_0, \dots, u_{L+2m-2} . A set of corresponding Greville abscissae can then be computed as the successive m -tuple averages of these knots. Given ordinates P_i (known as de Boor ordinates or control vertices) over the Greville abscissae, allows us to define the vertices of B-spline polygon B as the set of points $\{(\gamma_i, P_i)\}_{i=0}^{L+m-1}$.

Knot insertion inserts a real number $u \in [u_{m-1}, \dots, u_{L+m-1}]$ into the B-spline's domain knot sequence. The result is a new set of Greville abscissae γ_i^u , and correspondingly evaluated ordinates $P_i^u = B(\gamma_i^u)$. The points (γ_i^u, P_i^u) describe the refined B-spline polygon B^u , which contains one additional vertex compared to B , as seen in Figure 2.2. Specifically the refined B-spline curve is given by the knot sequence $u_0, \dots, u_I, u, u_{I+1}, \dots, u_{L+2m-2}$ for $n-1 \leq I < L+m-1$, and the

new control vertices P_i^u , which are computed using the knot insertion formula:

$$P_i^u = \frac{u_{i+m-1} - u}{u_{i+m-1} - u_{i-1}} P_{i-1} + \frac{u - u_{i-1}}{u_{i+m-1} - u_{i-1}} P_i,$$

$i = I - n + 2, \dots, I + 1$. To facilitate ease of representation and refinement evaluation, an alternate method known as blossoming [14] is often used to express the B-spline curve and its control points.

2.1.2 Knot Multiplicity

Knot multiplicity is the frequency of occurrence of a knot value in a knot vector. A B-spline curve over the domain knot interval $[u_{m-1}, \dots, u_{L+m-1}]$ has L domain intervals, and thus L curve segments when all domain knots have multiplicity one. In this case, each segment shares m control points with its neighbours and the B-spline curve is C^{m-1} continuous. However, if a domain knot is repeated, the number of domain intervals drop by one and the segment at the repeated knot shares one less control point with its neighbours. As a result the continuity at this knot reduces by one. In general, if a knot value u_i has multiplicity k , then a degree m B-spline curve is C^{m-k} at u_i ; this also holds for adjacent B-splines whose support contains u_i . A knot with multiplicity equal to the degree of its B-spline curve is said to have full multiplicity, and the curve is only guaranteed to be C^0 continuous at the associated point. If two adjacent knots have full multiplicity, then the B-spline control points for the curve over that interval are in fact Bézier control points. Consequently, when all the knots have full multiplicity, the B-spline is a piecewise Bézier curve having the Bernstein polynomials as the blending functions.

2.1.3 Curve Evaluation

One popular method for evaluating B-spline curves is known as the de Boor algorithm. It says that to evaluate an m -degree B-spline curve at a parameter value u , we need to insert u into the associated knot sequence until it has full multiplicity m . The resulting point position is the desired function value. In the case that u is already an element of the knot sequence, with multiplicity r , only $m - r$ additional insertions are required; typically $r = 0$. Formally, for

$u \in [u_I, u_{I+1}) \subset [u_{m-1}, u_{L+m-1}]$, $k = 1, \dots, m - r$, and $i = I - m + k + 1, \dots, I - r + 1$,

$$P_i^{u(k)} = \frac{u_{i+m-k} - u}{u_{i+m-k} - u_{i-1}} P_{i-1}^{u(k-1)} + \frac{u - u_{i-1}}{u_{i+m-k} - u_{i-1}} P_i^{u(k-1)},$$

which gives, $C(u) = P_{I-r+1}^{u(n-r)}$.

The de Boor method also facilitates evaluation of curve derivatives. Repeated knot insertion is stopped one level short at u having multiplicity $m - 1$, leaving two control points that share the knot value u , $P_I^{u(m-1)}$ and $P_{I+1}^{u(m-1)}$. The derivative of C at u is then given as

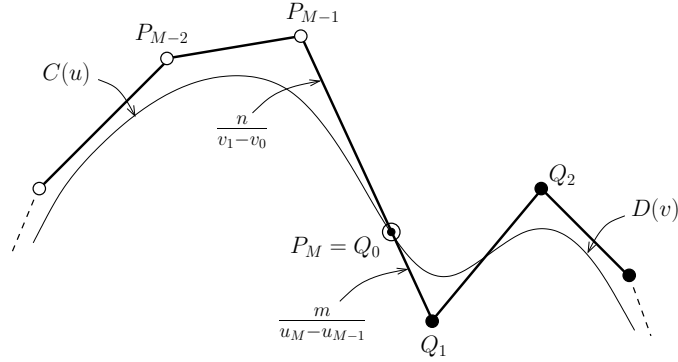
$$C'(u) = \frac{m}{u_{I+1} - u_I} (P_{I+1}^{u(m-1)} - P_I^{u(m-1)}).$$

2.1.4 Continuity

Two curves meet with C^k continuity at parameter value t if they agree in both position as well as in k derivatives at t . When establishing continuity, the two B-spline curves to be joined are often defined to have full end knot multiplicity. This places the beginning and end points of the curves at their first and last control points respectively, making it easier to set continuity. As an example, we state the C^0 and C^1 join conditions for two B-spline curves – m -degree $C(u)$ described by knots u_0, \dots, u_{M+m-1} and n -degree $D(v)$ described by knots v_0, \dots, v_{N+n-1} , each having full end knot multiplicity (illustrated in Figure 2.3). A C^0 join requires that the end point of C is also the start point of D . This can be achieved by setting $P_M = Q_0$. A C^1 join occurs when the curves meet with C^0 continuity and the first derivative at the end of C is equivalent to the first derivative at the beginning of D , here, $\frac{m}{u_M - u_{M-1}}(P_M - P_{M-1}) = \frac{n}{v_1 - v_0}(Q_1 - Q_0)$.

2.1.5 Closed Curves

A closed Bézier curve results when the two ends of a curve are joined by setting the first and last control points to be the same. A closed B-spline curve is obtained by establishing full continuity, C^{m-1} , between the two ends. For this, the last m control points of the curve need to be identical to the first m control points, and the corresponding knot spacings must also be equal. Given a cubic

Figure 2.3: B-spline Curves Joined with C^1 Continuity

B-spline represented by the knot vector $\{u_0, u_1, \dots, u_{M+2}\}$ and control points $\{P_0, P_1, \dots, P_M\}$, forming a closed B-spline curve involves satisfying the following set of constraints:

$$\begin{aligned}
 P_{M-2} &= P_0, \\
 P_{M-1} &= P_1, \\
 P_M &= P_2, \\
 u_{M+1} - u_{M+2} &= u_3 - u_4, \\
 u_M - u_{M+1} &= u_2 - u_3, \\
 u_{M-1} - u_M &= u_1 - u_2, \\
 u_{M-2} - u_{M-1} &= u_0 - u_1.
 \end{aligned}$$

Any modifications to the curve through knot insertion or otherwise, must be performed in a manner that maintains this closure relationship.

The valid domain knot interval over which a closed B-spline curve can be evaluated differs from its open curve analogue due to its cyclic construction. In an open B-spline curve, if the end knots are not of full multiplicity, some of the Greville points will not lie within the curve's valid range. To facilitate evaluation, the Greville points must either be clamped to the valid range or the end knots must be constructed to have full multiplicity. In the case of a closed B-spline curve we have

other options because the Greville points lying outside the valid interval get wrapped around. Closed curve evaluation can be performed either by swapping P_0 with P_{M-2} , or by starting at the second control vertex and evaluating over the interval from P_1 to P_{M-1} .

2.2 Tensor Product Surfaces

Tensor product surfaces are the result of extending curves to represent surfaces. A tensor product B-spline surface, S , is defined over a two-dimensional domain by a three-dimensional polygonal mesh of control points $P_{i,j}$ and their associated patch basis functions (Figure 2.4). The patch basis functions are obtained by taking the product of the two defining B-splines, $N^m(u)$ and $N^n(v)$, given in the u and v parametric domain directions respectively. Mathematically, we have

$$\begin{aligned}
 S(u, v) &= \sum_{i=0}^M \sum_{j=0}^N P_{i,j} N_i^m(u) N_j^n(v) \\
 &= \sum_{i=0}^M \left\{ \sum_{j=0}^N P_{i,j} N_i^m(u) \right\} N_j^n(v) \\
 &= \sum_{j=0}^N \left\{ \sum_{i=0}^M P_{i,j} N_i^n(v) \right\} N_j^m(u) \\
 &= \sum_{i=0}^M \sum_{j=0}^N P_{i,j} N_{i,j}(u, v),
 \end{aligned}$$

where $N_{i,j}(u, v) = N_i^m(u) N_j^n(v)$.

Evaluation of a tensor product surface involves performing repeated curve evaluation in one parametric direction and then the other. Essentially, we can apply the de Boor algorithm to all B-spline curves along the u (or v) direction to get control points describing a curve in v (or u), and then apply the de Boor algorithm to this curve to get the desired point on the surface. To simultaneously obtain the surface partials in both directions at the same point, a slightly modified algorithm given by Mann and DeRose [11] is used. The above evaluations are stopped one level short in both directions to produce a unit bicubic surface. Then, evaluating once in either direction, say u , gives the two control points describing the partial derivative $\partial \vec{v}$ along the

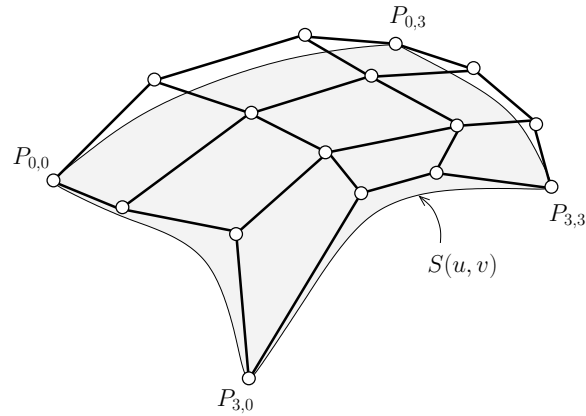


Figure 2.4: A Bicubic Tensor Product Patch with its defining control net

other parametric direction.

Continuity conditions for tensor product surfaces are based upon the continuity of the comprising B-spline curves. Joining these surfaces with a desired level of continuity requires extending rows or columns of control points such that the extension forms B-spline curves that satisfy the same level of continuity. It follows that for two surfaces to meet with C^1 continuity, the first two layers of control points along the join boundary of both surfaces must be colinear, and each cross-layer must form a curve that is C^1 continuous.

2.2.1 Tensor Product Cylinders

A tensor product cylinder (Figure 2.5) is a tensor product B-spline surface with its rectilinear domain defined to form a cylinder that has closed curve constraints placed on each of its circular layers. In my constructions and descriptions, the axis of the cylinder is along the u parametric direction, while each closed curve layer of control points is defined with respect to v .

2.3 Surface Pasting

Modelling frequently involves adding local detail to surfaces. The traditional method used for shape control of a tensor product B-spline surface is knot insertion. Unfortunately, this method

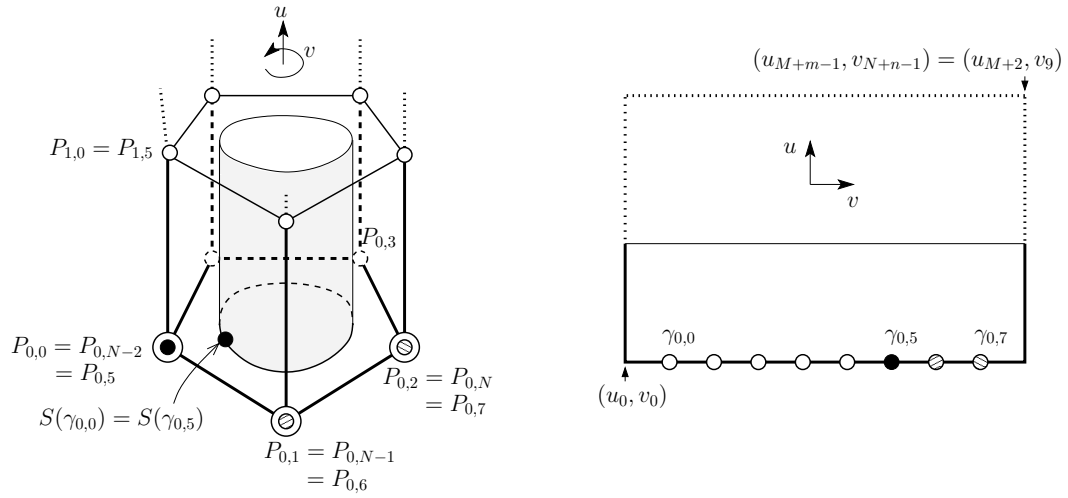


Figure 2.5: A Bicubic Tensor Product Cylinder – left: cylinder surface and its defining control net; right: 2D cylinder domain

adds significant surface complexity by creating extra subpatches across the entire width/breadth of the surface, instead of offering only the local refinement desired. Alternatives have included the use of hierarchical B-splines [8], wavelets [16], displacement maps [7] and surface pasting. Surface pasting offers some notable advantages over the other methods, including lower computational costs, minimal increase in storage requirements, flexibility of non-parametric alignments, easy repositioning, and reuse of surface details.

Introduced by Bartels and Forsey [3], surface pasting forms the foundation for the work in this thesis. The technique is a generalization of hierarchical B-splines, developed to combine the flexibility of displacement mapping with the speed of evaluation enjoyed by hierarchical B-splines. It involves adding detail to a region of one tensor product B-spline surface (designated as the base) by attaching a second tensor product surface (called the feature) to it. The base surface can be either a simple surface or a composite formed by previous pasting operations. The pasting procedure essentially adjusts the feature control points such that the boundary of the pasted feature lies on or near the base surface. The resulting feature is modified to reflect the topology of its underlying base, while still retaining characteristics of its original unpasted form; the base itself remains unchanged.

The surface pasting process makes use of two concepts – diffuse coordinate spaces and Greville displacement surface representations. The following subsections explain these concepts, building upon them to provide a detailed description of standard surface pasting [1, 2] as well as its cylindrical pasting [12, 13] extension.

2.3.1 Diffuse Coordinate Space

In a diffuse coordinate space, each control point $P_{i,j}$ is associated with a local coordinate frame $\mathcal{F}_{i,j}$. This provides an alternate way of expressing each feature control point as the frame origin $\mathcal{O}_{i,j}$, plus a displacement vector $\vec{d}_{i,j}$ given along local coordinate directions $\{\vec{x}_{i,j}, \vec{y}_{i,j}, \vec{z}_{i,j}\}$, i.e.,

$$P_{i,j} = \mathcal{O}_{i,j} + \vec{d}_{i,j}.$$

In surface pasting, the selection of the origin and displacement vectors for each control point affects the quality and behaviour of the pasted surface. To determine these values, a Greville displacement representation of the surface is used.

2.3.2 Greville Displacement

Greville displacement involves embedding the domain of a surface into its range space by mapping each domain point (u, v) to $(u, v, 0)$. Applying Greville displacement to a tensor product B-spline surface enables us to associate a local coordinate frame with each surface control point.

Tensor product construction ensures that each control point $P_{i,j}$ has an associated domain point at which it maximally influences the surface. This domain point is referred to as the Greville point $\gamma_{i,j} = (\gamma_i, \gamma_j)$, where γ_i is the i^{th} Greville abscissa in the u parametric direction and γ_j is the j^{th} Greville abscissa in the v direction. Embedding the Greville point into the range to give $\Gamma_{i,j} = (\gamma_{i,j}, 0)$, provides a point of origin for $P_{i,j}$'s local coordinate frame. Then, the displacement vector from $\Gamma_{i,j}$ to $P_{i,j}$ forms the corresponding Greville displacement $\vec{d}_{i,j} = P_{i,j} - \Gamma_{i,j}$. Consequently, a diffuse representation of a tensor product B-spline surface can be

formulated as

$$S(u, v) = \sum_{i=0}^M \sum_{j=0}^N (\Gamma_{i,j} + \vec{d}_{i,j}) N_{i,j}(u, v).$$

Now, we define each $P_{i,j}$'s local coordinate frame $\mathcal{F}_{i,j} = \{\vec{x}_{i,j}, \vec{y}_{i,j}, \vec{z}_{i,j}, \Gamma_{i,j}\}$, where the basis vectors $\vec{x}_{i,j}, \vec{y}_{i,j}$ are the u and v parametric directions of the embedded domain respectively, and $\vec{z}_{i,j} = (0, 0, 1)$. This allows us to express the Greville displacements relative to their corresponding local frames as

$$\vec{d}_{i,j} = d_{i,j}^x \vec{x}_{i,j} + d_{i,j}^y \vec{y}_{i,j} + d_{i,j}^z \vec{z}_{i,j},$$

where $d_{i,j}^x, d_{i,j}^y$, and $d_{i,j}^z$ are the scalar components of $\vec{d}_{i,j}$.

2.3.3 Standard Pasting

Surface pasting generates a hierarchical tensor product B-spline surface by pasting a feature onto a base surface. Each surface involved is defined over its own domain. As mentioned earlier, the process maps feature control points onto the base in an attempt to join the feature smoothly to the base. The resulting transformed feature takes on characteristics of the base onto which it has been pasted, while simultaneously continuing to reflect its original unpasted form. To achieve this, the feature control points are represented using Greville displacements relative to the feature domain space. These points are then associated with corresponding base domain points. Finally, each feature control point is positioned within the base range space using appropriate continuity criteria.

More specifically, standard surface pasting [1, 2] is used to paste the boundary of a non-closed feature surface onto the surface of a base. The details are presented below and illustrated in Figure 2.6.

We begin with a feature surface F defined by control points $\{P_{i,j} \mid i = 0, \dots, M, j = 0, \dots, N\}$, and a base surface B . Having constructed a Greville displacement representation of F (as described in §2.3.2), the first step of the pasting process involves mapping the feature domain into the base domain using an invertible transformation T . T determines the relative size and placement of the feature surface with respect to the base, and is typically defined by the user. Under

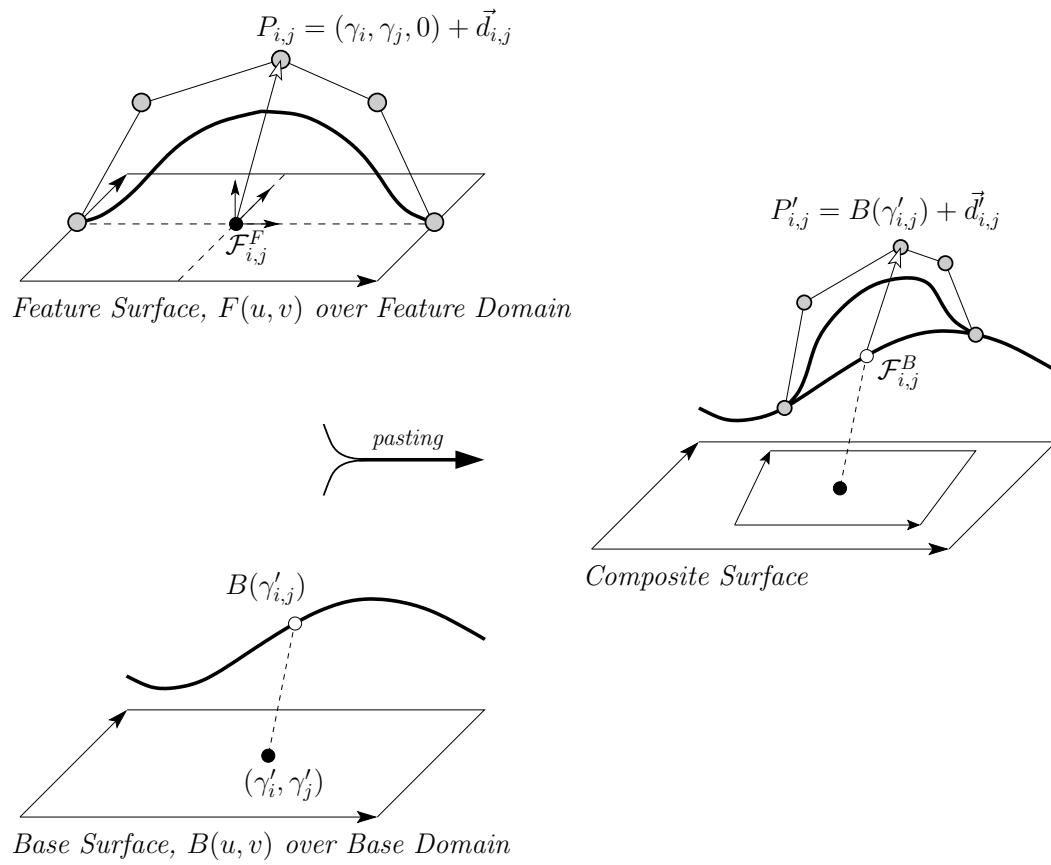


Figure 2.6: Standard Surface Pasting

T , each Greville point $\gamma_{i,j}$ is mapped to $T(\gamma_{i,j}) = T(\gamma_i, \gamma_j) = (\gamma'_i, \gamma'_j) = \gamma'_{i,j}$. The corresponding local coordinate frame $\mathcal{F}_{i,j}^F = \{\bar{x}_{i,j}, \bar{y}_{i,j}, \bar{z}_{i,j}, \Gamma_{i,j}\}$ is transformed as well – the origin is mapped to $\Gamma'_{i,j} = (\gamma'_i, \gamma'_j, 0)$ and the frame basis is mapped to $(\bar{x}'_{i,j}, \bar{y}'_{i,j}, \bar{z}'_{i,j})$, where $\bar{x}'_{i,j}$ and $\bar{y}'_{i,j}$ are the parametric directions of the embedded feature domain. As we are performing a two dimensional domain-to-domain mapping, we set $\bar{z}'_{i,j} = (0, 0, 1)$.

The next step is to create a base domain displacement representation of each feature control point. This is achieved by expressing each displacement $\bar{d}_{i,j}$ in terms of a local base coordinate frame $\mathcal{F}_{i,j}^B = (B(\gamma'_i, \gamma'_j), \bar{x}''_{i,j}, \bar{y}''_{i,j}, \bar{z}''_{i,j})$. Here, the origin is computed by evaluating the base at the transformed Greville point, and the frame basis is constructed to reflect curvature at this point using base surface directional derivatives at the origin. Therefore,

$$\begin{aligned}\bar{x}''_{i,j} &= \frac{\partial}{\partial \bar{x}'_{i,j}} B(\gamma'_{i,j}), \\ \bar{y}''_{i,j} &= \frac{\partial}{\partial \bar{y}'_{i,j}} B(\gamma'_{i,j}), \text{ and} \\ \bar{z}''_{i,j} &= \bar{x}''_{i,j} \times \bar{y}''_{i,j}.\end{aligned}$$

To position each feature control point on the base, its displacement vector is recomputed relative $\mathcal{F}_{i,j}^B$ as $\bar{d}_{i,j} = d_{i,j}^x \bar{x}''_{i,j} + d_{i,j}^y \bar{y}''_{i,j} + d_{i,j}^z \bar{z}''_{i,j}$.

The pasted control point locations can now be determined using point-vector addition, giving the pasted feature F^{pasted} as

$$\begin{aligned}F^{pasted}(u, v) &= \sum_{i=0}^M \sum_{j=0}^N P'_{i,j} N_{i,j}(u, v) \\ &= \sum_{i=0}^M \sum_{j=0}^N (B(\gamma'_{i,j}) + \bar{d}_{i,j}) N_{i,j}(u, v).\end{aligned}$$

It is important to note that surface pasting is only an approximation technique. Rather than mapping every point on the feature surface, only a small number of sample sites, the feature Greville points, are mapped. If the feature surface is described by too few control points or a coarse knot structure relative to the base, noticeable gaps at the join boundary may appear in

the composite surface. In general, there is no guaranteed continuity between feature and base surfaces.

In the case of standard surface pasting, C^0 continuity is approximated by defining the embedded feature domain in a manner that ensures all feature boundary control points coincide with their respective Greville points. Thus, $\vec{d}_{i,j}$ and $\vec{d}'_{i,j}$ must both equal zero for all $i = 0, M$ and $j = 0, N$, forcing the boundary control points to lie within the feature domain plane. As a result, the pasted feature boundary control points lie directly on the base surface. Provided the base has low curvature relative to the spacing between these points, a near C^0 join is achieved. This idea can be extended to approximate C^1 continuity as well, which requires that the cross-boundary derivatives of the feature be the same as base surface partials at corresponding locations under the pasted feature boundary.

Originally, standard surface pasting established a C^1 approximation by setting both the first and second boundary layers of feature control points to their corresponding Greville points, positioning both layers on the base surface. The vector difference between neighbouring base surface points of the two layers was deemed a reasonable estimate of the base's corresponding partial derivatives, assuming low curvature over the paste region. Cylindrical pasting, described in §2.3.4, introduced the idea of mapping the second layer of feature control points as displacements relative to the local coordinate frame of the associated first layer Greville point. The advantage of this approach is that it produces a surface with quadratic first derivative convergence, while with original pasting there was no possibility of such convergence. These ideas can also be extended to approximate higher levels of surface join continuity.

A standard method to improve the boundary approximations, thereby improving join continuity, is knot insertion. Inserting knots into the unpasted feature followed by repasting, progressively refines the approximation to within any desired tolerance. Unfortunately, the increase in storage and evaluation costs are rather significant, prompting an exploration of alternative ways to minimize the pasting discontinuities. The goal of such work has been to find better settings for the continuity affecting boundary layers of feature control points, while maintaining flexibility and keeping costs low. Notable improvements have been offered by techniques using

quasi-interpolation [4, 5] and least squares fitting [9, 10].

2.3.4 Cylindrical Pasting

Cylindrical surface pasting [12, 13] evolved due to the expected benefits of applying the surface pasting concept to a wider variety of modelling situations. It can be described as a technique that integrates parametric trimline-based blending to extend surface pasting [17]. Standard pasting only allows for the pasting of one open surface atop another. Cylindrical pasting offers a method for connecting two base surfaces using a cylinder to join them smoothly. The feature surface used must always be a tensor product cylinder having a representation given in §2.2.1. Essentially, two types of cylindrical pastes can occur – pasting of the cylinder’s end onto a base tensor product surface, or pasting end-to-end onto another cylinder. This thesis is concerned only with the former case, and the reader is referred to [12, 13] for further details on cylinder-to-cylinder pastes.

As with standard surface pasting, the feature control points are mapped relative to the base surface to produce a pasted feature surface that lies at the desired location. The difference is in the domain mapping and control point displacements used.

To paste one end of a tensor product cylinder C onto a base surface B (Figure 2.7), the corresponding edge of the feature domain is mapped to a circle in the base domain. Each cylinder control point along this paste edge, $\{P_{0,j}\}_{j=0}^{N-3}$, is located at its corresponding Greville point $\gamma_{0,j}$ in the embedded feature domain. This position is in turn associated with a point $t_j = (u_j^B, v_j^B)$ on the base domain circle, thereby mapping the boundary L_0 layer of cylinder control points onto the base surface. The t_j s selected are spaced evenly over the domain circle. The resulting pasted cylinder boundary lies close to, but not directly on, the base surface. This is taken to be an adequate approximation of C^0 continuity between feature and base. As with standard pasting, knot insertion can be used to improve this approximation.

To establish an approximate C^1 join, the next layer (L_1) of cylinder control points needs to be mapped onto the base as well. Effectively, we want to map the differences of the first two layers of control points, $P_{1,j} - P_{0,j}$, to cross-boundary derivatives of the base surface. This is achieved by constructing a coordinate frame $\mathcal{F}_{0,j}$ at each L_0 control point, with $P_{0,j}$ as the origin. The

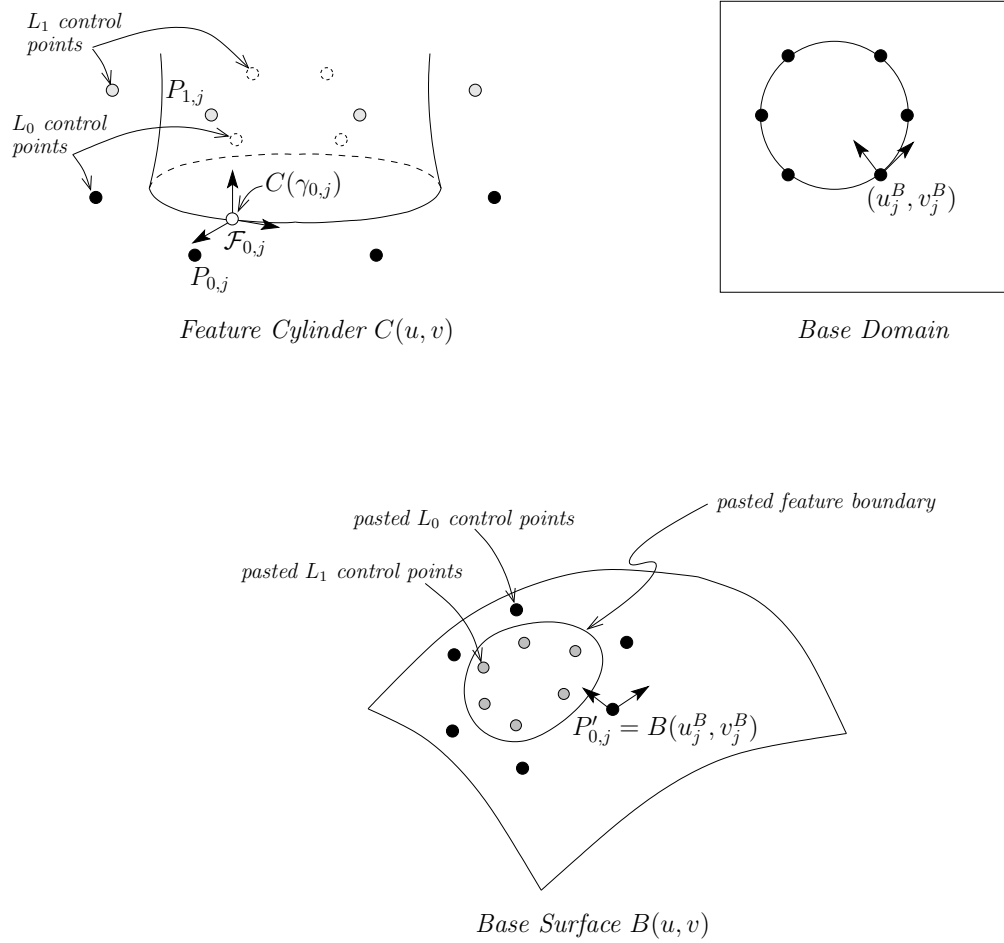


Figure 2.7: Cylindrical Pasting

basis vectors are the two unit derivative vectors in the corresponding u and v feature domain parametric directions and their cross-product. The first two coordinate directions are tangent to the unpasted feature and are mapped to the embedded base domain – the basis vector along v maps to be tangent to the base domain paste circle, while the basis vector along u maps to be perpendicular to the circle and inward pointing. This frame is then mapped onto the base surface giving $\mathcal{F}'_{0,j}$. Each L_1 control point $\{P_{1,j}\}_{j=0}^{N-3}$ can be expressed as a displacement relative $\mathcal{F}_{0,j}$. These displacements are accordingly used to weight the elements of $\mathcal{F}'_{0,j}$ to get the location of $P'_{1,j}$.

Now, although the cylindrical pasting process, i.e., mapping of the cylinder boundary onto the base, is complete, only the first two layers of pasted control points have been determined. While in standard pasting all feature control points have a well-defined placement relative to the base, in cylindrical pasting only the first two rows of cylinder control points involved in establishing continuity with the base have a clear association. The remaining control points must be mapped using other techniques such as spline interpolation, the details of which are not relevant to the work in this thesis.

Chapter 3

Towards Improving Cylindrical Pasting

3.1 Motivation and Goals

The many advantages of surface pasting over existing alternative methods make it a valuable interactive surface modelling technique. At the same time, the approximations used in this technique result in a design whereby a pasted feature is not guaranteed to meet its base surface with any order of continuity at the join boundary. In particular, undesirable gaps between surfaces appear when the pasted feature has a coarse knot structure or when the base has a high curvature. Feature refinement using knot insertion can partially alleviate this C^0 discontinuity by generating a set of control vertices that lie closer to and more accurately represent the actual surface boundary. Unfortunately, the resulting increase in feature control points needing to be mapped onto the base, directly translates to a higher boundary evaluation cost and additional storage requirements. Alternatives to minimize these discontinuities, while retaining the overall benefits of surface pasting, have been previously explored. Specifically, the methods used have been quasi-interpolation [4, 5], least squares approximation [9, 10], and Greville point interpolation [15]. However, these implementations suffer from high evaluation costs and/or significant algorithmic

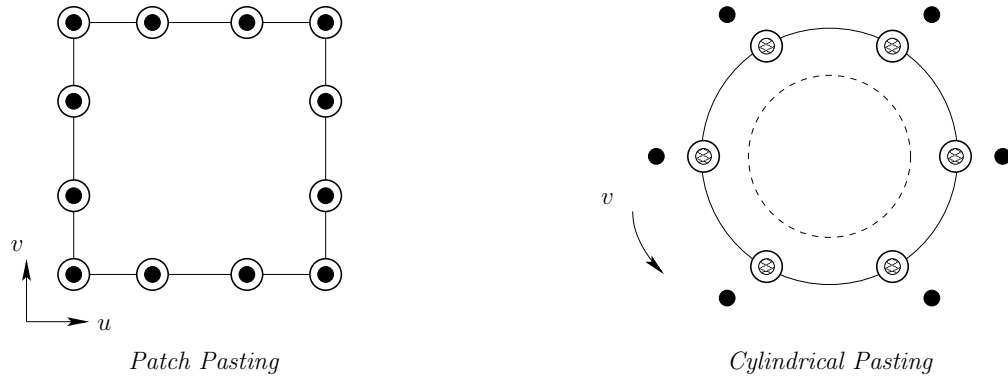


Figure 3.1: Approximations using zero Greville displacements – it is possible to define a patch with zero Greville displacement of edge control points, whereas in the case of a cylinder this approximation changes the defined curve

complexities. In this thesis, I develop and examine computationally simple and cheap algorithms, requiring little additional cost beyond surface evaluation to improve continuity, thereby keeping more in tune with the original spirit of surface pasting as a low-cost, rapid prototyping and previewing method [2].

The studies in this thesis are done in the context of cylindrical pasting. Standard patch pasting assumes that the feature’s boundary control points have zero displacement vectors with respect to their corresponding Greville points. This is a reasonable in the context of patch pasting as the control points describe a linear curve. Original cylindrical pasting by Mann and Yeung [12, 13] applied this same concept to the C^0 layer of a feature cylinder. However, while zero displacement control points reproduce the linear boundary of a standard patch, placing the control points on

the boundary of a closed curve does not reproduce the closed curve (Figure 3.1). Therefore, in this thesis I explore more true, yet simple and low-cost, C^0 closed curve approximating alternatives for cylindrical pasting. As there is presently no clearly established, widely acceptable, standard method for cylindrical pasting, it is hoped that the results from my experimentation will yield a suitable standard that could later be carried over to and examined for a more generic patch pasting as well.

The cylindrical pasting methods proposed and examined here focus only upon improving the approximation of the boundary continuity (i.e., C^0 continuity) between the pasted feature cylinder and its underlying base surface. The newer techniques attempt to place the pasted cylinder control vertices more intelligently than a direct application of standard pasting, hoping to improve the resulting trim curve approximation and reduce composite surface discontinuities without needing to resort to feature refinement. In a more generic sense, the work attempts to find a low-cost method of using a given closed B-spline curve to approximate a different given closed curve with minimal reproduction error. The implications of these techniques with respect to the improved accuracy of cross-boundary derivative evaluations used for establishing C^1 continuity are not studied here. However, my results may provide some insight on potential directions for their improvement as well.

3.2 Basics

Pasting one edge of a cylinder onto a base surface is accomplished via a domain space mapping, as detailed in §2.3.4. I have experimented with variations on ways to perform this mapping. In particular, four algorithmically simple and computationally inexpensive alternatives along with two minor variations of these methods are explored and compared in this thesis.

The method discussions assume that a given $m \times n$ tensor product feature cylinder $C(u, v) = \sum_{i=0}^M \sum_{j=0}^N P_{i,j} N_{i,j}(u, v)$ is being pasted onto the surface of a tensor product base $B(u, v)$ along the cylinder paste edge $L_0 : u = u_0$. The resulting pasted feature boundary is constructed as an approximation to a curve on the base surface called the trim curve. This trim curve

is given by a user-defined circular paste curve within the base domain. A polynomial paste curve could be used instead, however, starting with a circular representation provides reasonable paste-quality comparisons while allowing for simpler implementations. If a particular method appears promising, its behaviour for non-circular paste curves can be assessed by adjusting the implementations for center-and-radius circles described below to alternatively work with B-spline curves within the same base domain (Appendix A).

3.3 Greville Paste

The Greville Paste method is similar in concept to the technique described in the original work on cylindrical pasting. It assumes that the cylinder's boundary control points lie on the cylinder's surface boundary curve itself, clamping the Greville displacement vectors to zero. This approximation allows for a simplistic paste involving mapping of the boundary Greville points onto the base surface, followed by placement of corresponding control points at these mapped locations. The process is best understood in the context of Figure 3.2.

To perform a Greville Paste, the feature cylinder's L_0 surface Greville points $\{C(\gamma_{0,j})\}_{j=0}^{N-3}$, are first embedded into the base domain. This is achieved by a simple placement of the $\gamma_{0,j}$ s onto paste points t_j given on the paste curve within the 2D uv -plane of the base domain. Specifically, these paste points are determined in proportion to the v -interval of the cylinder's domain. Choosing a circular paste curve for experimentation purposes makes the selection of paste points straightforward. $\gamma_{0,0}$ is mapped to t_0 , which is chosen relative to the centre of the paste curve circle at an angle of zero degrees to the u -parametric direction of the base domain. This gives the embedded Greville point $\gamma'_{0,0}$ located at t_0 . Computing $\theta = 2\pi/(\gamma_{0,N-2} - \gamma_{0,0})$, the remaining $N - 3$ $\gamma'_{0,j} = t_j$ points are similarly set at angles $\theta_j = (\gamma_{0,j} - \gamma_{0,0}) \times \theta$. Initial paste points, referred to as the set $\{t_j\}_{j=0}^{N-3}$, are generated in this manner for all the cylindrical pasting methods presented in this thesis.

A de Boor surface evaluation of the base at each embedded Greville point $\gamma'_{0,j}$, gives the mapped location of the cylinder's pasted L_0 surface Greville points lying on the base surface as

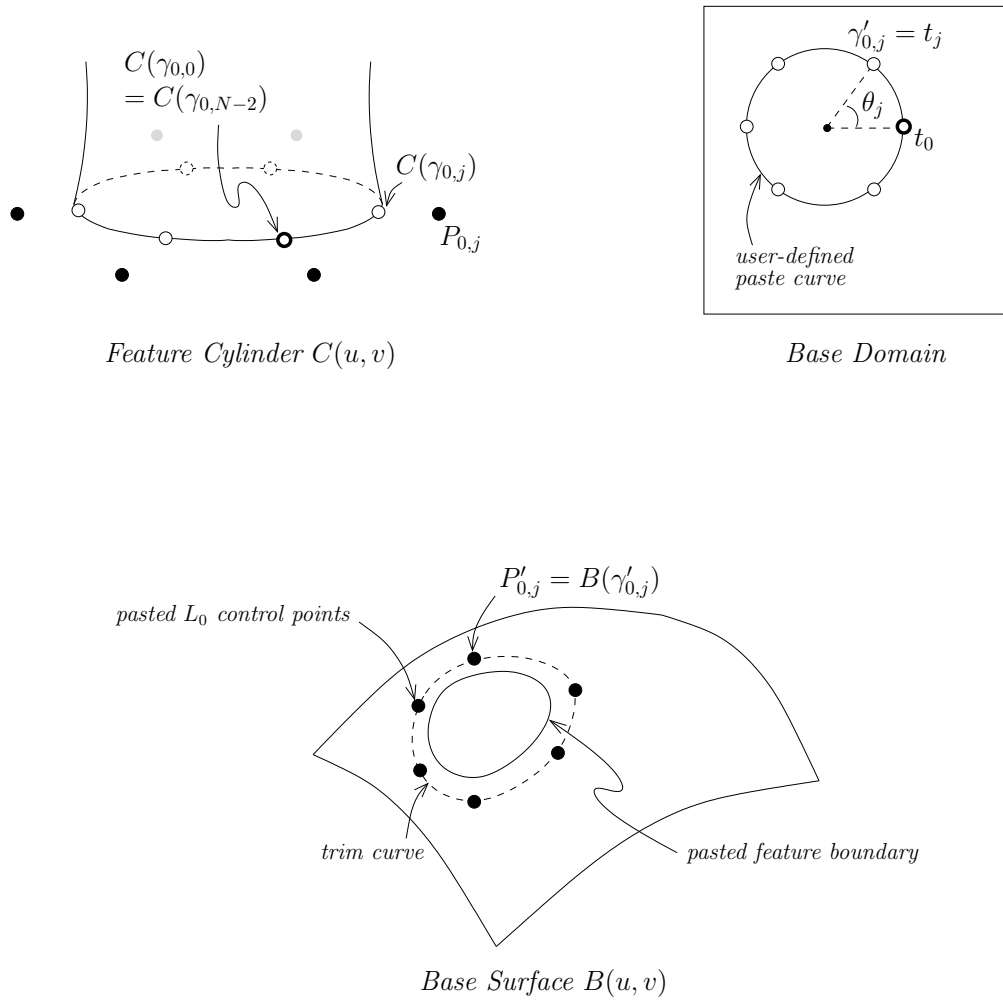


Figure 3.2: Greville Paste

$\{B(\gamma'_{0,j})\}_{j=0}^{N-3}$. Finally the L_0 feature control points are set to lie at the pasted Greville points with a zero displacement. The result is a set of pasted control points $P'_{0,j} = B(\gamma'_{0,j})$, which together describe the pasted cylinder boundary.

The cylinder $P'_{0,j}$ generated by the Greville Paste method always lie on the base surface as well as on the trim curve. However, the resulting pasted cylinder's closed curve boundary will always lie completely inside the convex hull given by these points. Consequently, gaps between the pasted feature boundary and trim curve are inevitable with this method. Further, pasting over any non-planar region is sure to reveal gaps between the base surface and pasted cylinder edge.

Although this cylindrical pasting C^0 continuity approximation seems less than acceptable, the Greville Paste method provides useful error and cost bounds, making it suitable as a comparative base case method. In particular, one can expect its application to yield

1. a comparative evaluation cost metric – the only computation involved in determining the pasted feature produced by a Greville Paste is one surface evaluation for each boundary control vertex
2. a maximum acceptable error bound – alternate methods should offer a reduction in error to offset their higher expected computational costs
3. a well-defined convergence – upon infinite refinement, the pasted control vertices will in fact define the trim curve.

3.4 Control Point Paste

Control Point Paste is the first of three new cylindrical pasting techniques I have devised, with the goal being to position the pasted cylinder edge on top of the base surface trim curve as accurately as possible by mapping a truer representation of the feature cylinder.

When computing a paste, the Control Point Paste method attempts to account for the non-zero Greville displacement between the cylinder control points and their corresponding surface Greville points. Specifically, the embedded location of each cylinder control point within the base

domain is determined as the sum of associated embedded Greville points and transformed Greville displacement vectors. The implementation specifics, illustrated in Figure 3.3, are detailed below.

Given the tensor product feature cylinder C , the first step of a Control Point Paste is to determine the L_0 Greville displacement vectors. For each control point $P_{0,j}$, the displacement vector \vec{d}_j is computed with respect to a unique local coordinate frame F_j constructed such that,

- F_j^O , the origin of F_j , is at its corresponding surface Greville point, and is obtained by evaluating the feature surface at the associated Greville abscissa: $F_j^O = C(\gamma_{0,j})$
- \hat{F}_j^x is given by a unit normal in the direction of the difference vector between the surface Greville point and the centre of the cylinder's L_0 edge; the boundary curve's centre, C_c , is simply determined using Ceva's Theorem [18] by taking the evenly weighted barycentre of the polygon vertices given by the surface Greville points: $\hat{F}_j^x = \frac{F_j^O - C_c}{|F_j^O - C_c|}$
- \hat{F}_j^y is given by the normalized tangent to the cylinder's boundary curve at the chosen origin, and is along the v -parametric direction; this is also the directional derivative obtained by a de Boor evaluation of the L_0 curve
- \hat{F}_j^z is given by a unit vector perpendicular to both \hat{F}_j^x and \hat{F}_j^y .

The coordinates of each control point in relation to this local frame give the xyz components of the Greville displacements. By construction, the tensor product cylinders used in this thesis are such that the control points within each u -layer are coplanar, therefore the d_j^z s will be zero.

The initial paste points t_j on the paste curve given in the base domain are determined as they were for the Greville Paste method. As the paste curve represents the ideal pasted cylinder boundary, these initial points can be seen as locations where the L_0 surface Greville points would lie. Using the Greville displacements, it is then possible to compute the relative control point paste locations within the base domain space. In particular, \hat{F}_j^x is mapped to \hat{s}_j^x , the out direction at t_j given by the 2D difference vector between t_j and the circular paste curve's centre point. \hat{F}_j^y maps to \hat{s}_j^y along the tangent to the paste curve at t_j . To account for the space change, a scale factor α , equal to the ratio of paste curve to cylinder curve radii is used. Applying the proportional displacement gives the paste points p_j within the base domain. De Boor evaluations at the p_j s

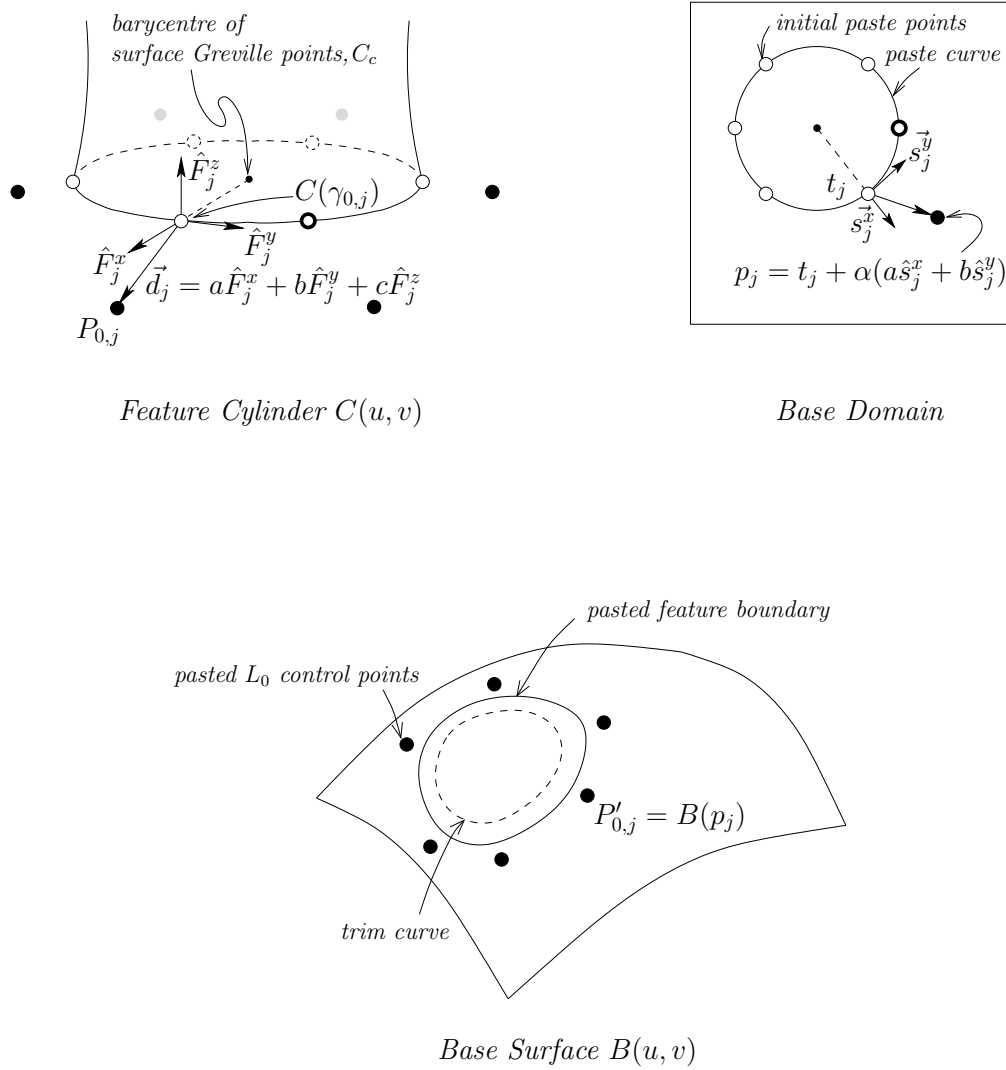


Figure 3.3: Control Point Paste

produce the set of pasted control points describing the Control Point pasted cylinder boundary, $P'_{0,j} = B(p_j)$.

Applying a 3D displacement within a 2D domain space results in pasted control points that lie on the base surface; however the resulting pasted cylinder edge is unlikely to lie on the base unless the paste region is planar. A potential way to avoid errors introduced by the 3D-in-2D computations is to account for the feature's L_0 Greville displacements in the 3D base range space instead. This alternative is explored using the next method.

3.5 Directional Displacement Paste

Directional Displacement Paste attempts to reduce C^0 gaps by computing the pasted control point locations in the base range space rather than in the base domain space. Representative points on the desired trim curve, i.e., paste curve paste points mapped into the base range space, are used to determine the placements. The relative positioning is computed using feature L_0 Greville displacements in a manner that retains defining characteristics of the feature cylinder, while simultaneously establishing a direct relationship to the trim curve on the base surface. The details, in context of Figure 3.4, follow.

Evaluating the base surface at points t_j generates a set of points t'_j lying on the trim curve. The trim curve is a mapping of the paste curve into the base range space. Ideally, the pasted cylinder boundary will be placed exactly on top of this trim curve. This in turn suggests that the pasted cylinder edge should be constructed such that all the trim points t'_j lie on it. By definition, surface Greville points lie on the surface they describe. Therefore, Directional Displacement maps the L_0 surface Greville points onto the base surface trim points. The pasted L_0 cylinder control points are then computed by placing them relative to these pasted Greville point locations. The displacements are determined by the cylinder's L_0 Greville displacement vectors \vec{d}_j , which are mapped through the base domain onto the base surface.

The computation of Greville displacements is as described for Control Point Paste (§3.4) giving,

$$\vec{d}_j = a\hat{F}_j^x + b\hat{F}_j^y + c\hat{F}_j^z, \text{ where } c = 0.$$

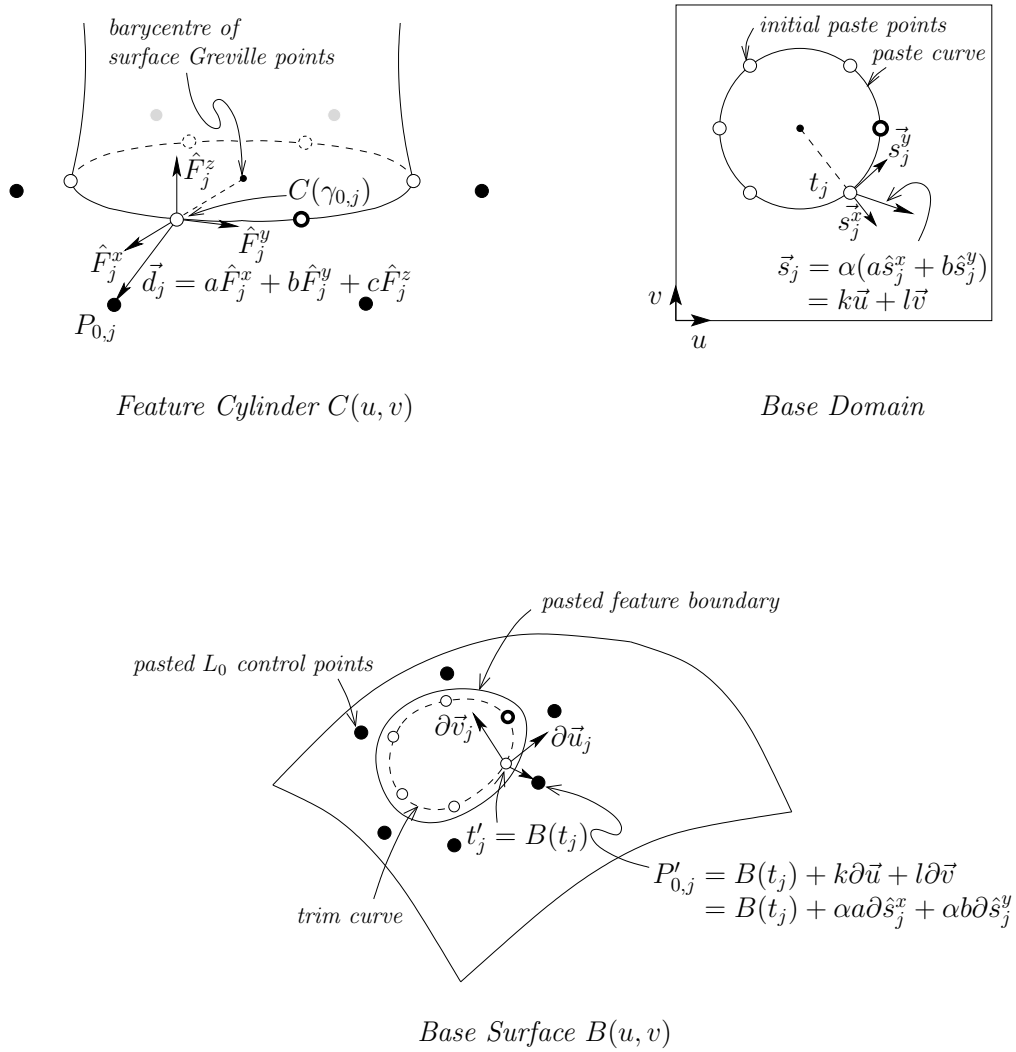


Figure 3.4: Directional Displacement Paste (Local)

Mapping each displacement \vec{d}_j involves first determining the pre-image of its components within the base domain space. The directional associations are \hat{F}_j^x along the out vector at t_j , and \hat{F}_j^y along the tangent to the paste curve at t_j . The space change scale factor α , as given in §3.4, is used to adjust the transformed vector length.

Next, relating the embedded displacement $\vec{s}_j = \alpha(a\hat{s}_j^x + b\hat{s}_j^y) = k\vec{u} + l\vec{v}$ to its image on the base surface is achieved using the base surface directional derivatives at the image of corresponding cylinder Greville points t'_j . A Mann-DeRose base surface evaluation at t_j gives the partial derivatives along the uv base domain directions, in addition to giving t'_j . The base uv -components of $a\hat{s}_j^x$ and $b\hat{s}_j^y$, i.e., k and l are used to weight these uv -directional vectors respectively, giving a Greville displacement $k\partial\vec{u} + l\partial\vec{v} = \alpha a\partial\hat{s}_j^x + \alpha b\partial\hat{s}_j^y$ within the base range space. A point-vector addition of transformed feature-to-base space L_0 Greville points and Greville displacements, gives the Directional Displacement pasted cylinder boundary control points.

A potentially useful modification to Directional Displacement Paste came about from observing the performance of the above described method on initial test data. Over a hump-like paste region, the high surface curvature at the trim points displaced the control points in a manner that pushed the pasted feature boundary well below the base surface trim curve. As a result, I decided to examine the pasting behaviour when a simple form of average surface curvature over the paste region is used instead of local curvature displacements for this method.

To incorporate an average surface curvature, a mapping of the paste curve centre point onto the base, and computation of base surface directional derivatives at it, are performed using a Mann-DeRose evaluation. The pasted boundary control point locations are then determined by applying the corresponding Greville displacement vector components along the centre point's uv -directional vectors. The local directional derivatives at each t'_j no longer need to be computed. Preliminary tests demonstrated that this modified method merits further examination, although it is expected that when pasting over a region of surface inflection the averaging benefits will break down and higher errors than those produced by the local alternative will result. For the remainder of this thesis, the original technique is referred to as Local Directional Displacement Paste, and the modified method is termed Average Directional Displacement Paste.

3.6 Relative Displacement Paste

Relative Displacement Paste is motivated by Directional Displacement Paste. It too attempts to compute the L_0 pasted cylinder control points by accounting for the Greville displacements in the base range space as opposed to the base domain space. The difference is in how the displacement frame is constructed at each mapped cylinder Greville point on the base. Directional Displacement determines a mapping of each original Greville displacement frame F_j into the 2D base domain space, and applies the Greville displacements \vec{d}_j relative this s_j frame (Figure 3.4). However, as the shape of the cylinder's L_0 boundary curve distorts with pasting, the relationship of the pasting displacement frame directions to the feature boundary points end up changing as well. Relative Displacement Paste instead determines the pasting displacement frames such that the original F_j relationships to the feature boundary are maintained. It seems worth exploring whether maintaining the displacement relationship between cylinder surface Greville points and control points in this manner will produce a better approximation to the desired trim curve.

Method details are described below in relation to Figure 3.5. For all $j = \{0, \dots, N - 3\}$, F_j , \vec{d}_j , $\gamma'_{0,j} = t_j$, and $B(\gamma'_{0,j}) = t'_j$ are computed exactly as for Directional Displacement Paste (§3.5). The pasting displacement frame S_j at each t'_j is constructed such that,

- \hat{S}_j^x is the unit difference vector between t'_j and the new barycentre of pasted Greville points
- \hat{S}_j^y is the normalized tangent to the trim curve at t'_j , given by the difference of slopes between t'_j and its two neighbouring pasted Greville points.

The local frame directions \hat{F}_j^x and \hat{F}_j^y are now mapped to \hat{S}_j^x and \hat{S}_j^y respectively. The Greville displacement components a and b determined using $\vec{d}_j = a\hat{F}_j^x + b\hat{F}_j^y + 0\hat{F}_j^z$, are applied to the two new S_j frame directions to give a similar control point placement relative t'_j . A change of space scale factor β is applied to the displacement vector to account for the transformation from feature surface space to base surface space. β is computed as the ratio of the average distance between original L_0 surface Greville points and their barycentre to the average distance between pasted surface Greville points and their barycentre.

Two variations of Relative Displacement Paste are examined in this thesis. They differ in the

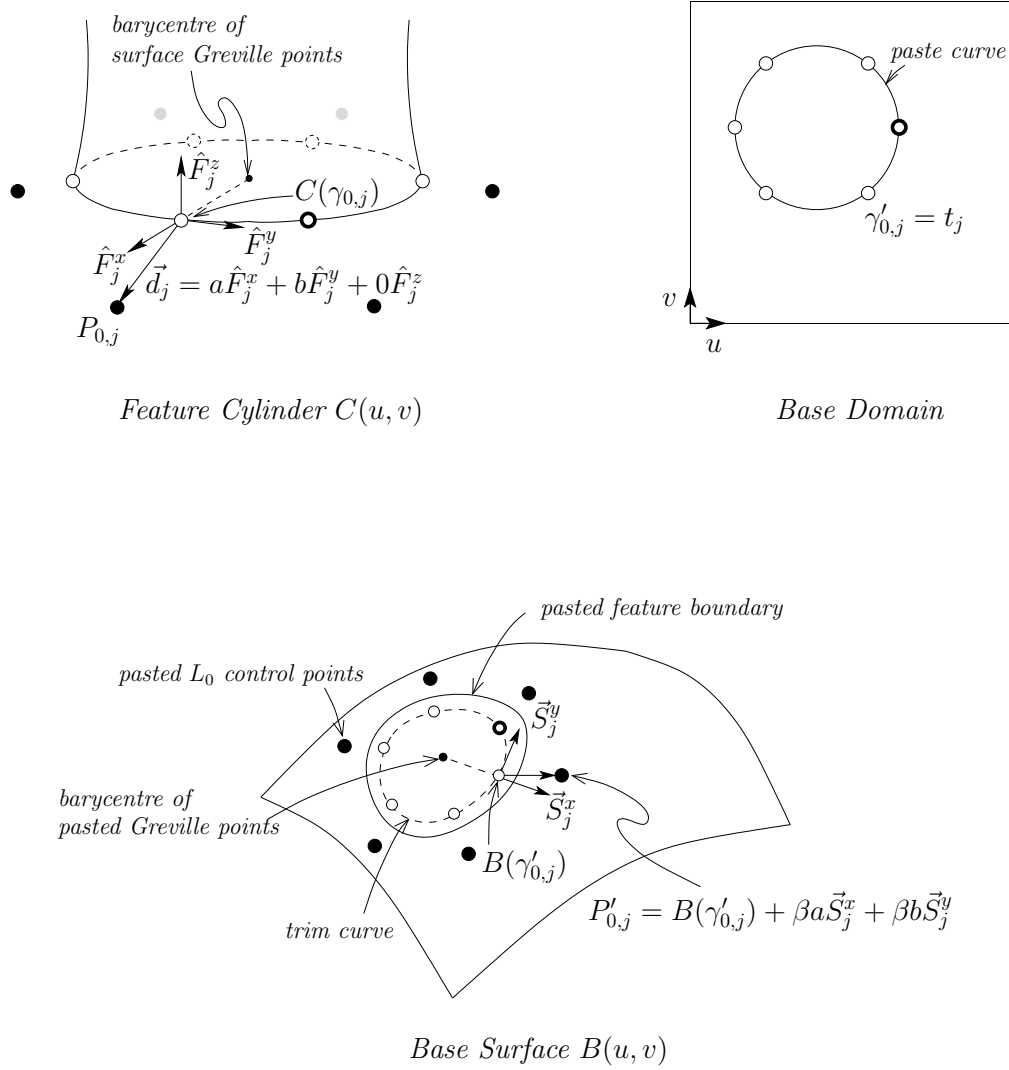


Figure 3.5: Relative Displacement Paste (Average)

computation of the pasting out vector \vec{S}_j^x for each pasted Greville point. The Average Relative Displacement method uses the barycentre of all $\{t'_j\}_{j=0}^{N-3}$, whereas the Local Relative Displacement method uses a local barycentre given by t'_j and its two neighbouring pasted Greville points to determine the direction. The idea being that when the curvature of a base surface has more noticeable variations over the paste region boundary, locally affected \vec{S}_j^x s may offer a better placement of the control points.

3.7 Computational Analysis

One of my primary considerations in the construction of C^0 cylindrical pasting algorithms described in this chapter was to keep computational costs and complexities low, while still attempting to reduce boundary gaps at the surface joins. Surface pasting is expected to offer interactive modelling, therefore, the adoption of a particular cylindrical pasting method requires that it not be noticeably more expensive than applying traditional pasting to cylinders. This section compares the costs of pasting a $m \times n$ feature cylinder $C(u, v) = \sum_{i=0}^M \sum_{j=0}^N P_{i,j} N_{i,j}(u, v)$ onto a base surface using each method.

The most significant computational cost in surface pasting is the number of base surface evaluations that need to be performed to position the feature's pasted control points. One surface position evaluation per L_0 cylinder control point is the minimum C^0 requirement for any cylindrical pasting method. An approximation improvement technique such as knot insertion rapidly becomes unacceptable as it doubles the number of control points at each level of refinement, thereby increasing evaluation costs exponentially. I have attempted to find ways to improve pasted boundary approximations of the trim curve for relatively small increases in cost. To keep the relative costs in perspective, a de Boor position-only surface evaluation for a bicubic tensor product surface requires 30 affine combinations, a Mann-DeRose position-with-derivatives evaluation takes 37 affine combinations, and a vector difference of a pair of points is one affine combination.

Greville Paste is essentially a direct application of standard surface pasting to cylindrical

features and requires only the bare minimum computation – one base surface evaluation for each L_0 cylinder control point, for a total of $N - 3$ position-only evaluations.

All the other methods I have explored account for the non-zero Greville displacement between surface Greville points and corresponding control points. Determining this displacement involves setting up of a local coordinate frame at each feature surface Greville point. This requires a position plus derivative de Boor curve evaluation of the cylinder boundary to obtain each origin surface Greville point and the tangent direction at it. A vector difference of two points within the plane of surface Greville points and control points gives the other non-zero displacement frame direction. To offer a cost comparison, for a degree $m \times 3$ tensor product feature cylinder, computing the Greville displacement takes 9 affine combinations per control point. Finally, given a mapped cylinder Greville point location, the vector sum of the two displacement components is used to place the control point. For the remainder of this computational analysis section I will refer to this set of costs as the displacement evaluation cost.

A Control Point Paste takes one displacement evaluation in addition to one position-only base surface evaluation for each of the $N - 3$ control points being pasted. The cost of a Local Directional Displacement Paste is somewhat higher, as a position-with-derivatives surface evaluation must be performed for each control point along with a displacement evaluation. Comparatively, an Average Directional Displacement Paste requires one additional base surface evaluation at the feature boundary's barycentre point, however, the directional derivatives only need to be computed at this one point as opposed to all the L_0 control points. As for the Relative Displacement Pastes, both types require the basic position-only surface evaluation, a displacement evaluation, as well as the determination of a new pasting displacement frame for each cylinder boundary control point. Establishing the pasting displacement frame consisting of tangent and out direction vectors at each pasted Greville point takes 3 additional affine combinations. Local Relative Displacement uses one further vector difference calculation per control point to determine its change of space scaling factor.

The evaluation cost per control point increases slightly for all cases when the paste curve within the base domain is given as a closed B-spline curve, rather than a circle with centre and

Method	Affine combinations per control point
Greville Paste	30
Control Point Paste	40
Local Directional Displacement	47
Average Directional Displacement	$40 + \frac{37}{N-3}, N \geq 9$
Local Relative Displacement	44
Average Relative Displacement	43

Table 3.1: Costs of pasting a $m \times 3$ cylinder onto a bicubic patch

radius. Determining the paste point then involves a de Boor paste curve evaluation, a small increase in cost since the curve is likely to be cubic. This additional computation becomes a part of the minimum evaluation cost per control point. The special cylindrical pasting methods requiring displacement calculations within the base domain space end up using two further affine combinations to obtain the tangent and out vectors at the paste point for this polynomial paste curve.

A comparative summary of the costs per control point, as assessed above, is given in Table 3.1; the values specified are for a cylindrical paste onto a circular paste curve. Essentially, the cost of pasting a control point using any of the methods tested in this thesis is at most half as expensive as doubling the number of control points using knot insertion to improve the pasted join accuracy.

3.8 Error Bounds

To provide a bound on how fast the error in C^0 continuity is expected to converge with feature cylinder refinement, I shall use the concept of linear reproduction. Given a polynomial function F and its approximation P , a Taylor series expansion gives the error as $\sum_{i=0}^{\infty} \frac{F^{(i)}(\xi) - P^{(i)}(\xi)}{i!} h^i$. An interpolation method is said to have linear precision if $F(\xi) = P(\xi)$ and $F'(\xi) = P'(\xi)$. In this case, the first two terms of the Taylor series cancel, leaving an error of $\sum_{i=2}^{\infty} \frac{F^{(i)}(\xi) - P^{(i)}(\xi)}{i!} h^i = O(h^2)$, where h is the distance between samples. Standard surface pasting is expected to have this property, as was verified empirically by Conrad [4].

To theoretically determine whether the above properties hold for the cylindrical pasting meth-

ods in this thesis requires two presuppositions. Firstly, from Taylor series analysis, if a curve is approximated using a function that has linear precision, then second order convergence is expected if certain conditions hold. Likewise, if a surface approximation has linear reproduction, we again obtain second order convergence. Now, say we have a closed curve C that lies on a surface, and C is approximated by a closed curve F where F reproduces C when the surface is a linear surface. Based upon the individual curve and surface approximation behaviours, I conjecture that the method generating F as an approximation to C will have second order error convergence. However, I am unaware of a theorem giving this result. Secondly, cylindrical pasting is an approximation method while the Taylor series result is only established for interpolation methods. However, over sufficiently small sampling intervals h , a curve approximation can be taken to be an interpolation between the two sample points. This allows us to apply linear reproduction properties to cylindrical pasting methods producing a pasted feature boundary curve as an approximation to the base surface trim curve.

Conceptually, linear reproduction in the context of surface pasting would suggest that the pasted curve on a planar base is the exact image of the domain curve representing it. Here, the domain curve is obtained by mapping the feature boundary into the base domain, and the image of its associated domain control points on the base describe the pasted boundary. One possible way to ascertain whether this property holds for each of the cylindrical boundary pasting schemes presented in this thesis is to show that the pasted cylinder's boundary is identical to its trim curve for a linear base surface. The comparison requires that the cylinder boundary and trim curve have the same representation in terms of degree and knot vector, as well as that both curves are parametrically aligned. The analyses make use of an affine geometry result that says, if we have a B-spline curve and corresponding control points, their affine map reproduces the same curve, i.e., $B(\sum P_i N_i(u)) = \sum B(P_i) N_i(u)$.

Greville Paste: This scheme places the boundary control points on the paste curve, not at control point locations describing the paste curve. Therefore, the boundary points are mapped to positions that will be different from the trim points. Consequently, Greville Paste can not be said to have linear reproduction.

Control Point Paste: Under the preconditions of common representation and alignment of boundary and trim curves, evaluation of boundary control point locations within the base domain by taking the paste curve as the boundary curve gives us the paste curve control points themselves. Therefore, both the pasted boundary and the trim curve are represented by the same set of base domain control points. These can be mapped affinely to produce the same curve, and are affected only by a common scale factor when placed onto the base surface. This indicates that Control Point Paste should indeed have linear reproduction.

Directional Displacement Paste: Examining the linear case of this method using the \vec{s} frame partials rather than the uv partials of Figure 3.4, we have

$$B(\sum(t_i + \vec{s}_i)N_i(t)) = \sum(B(t_i)N_i(t) + B(\vec{s}_i)N_i(t)).$$

This essentially says that each pasted boundary control point obtained by adding the corresponding base surface Greville displacement to its base trim point, is identical to the base surface point given by applying the displacement and locating the control point within the base domain. This equality means that this method satisfies linearity. This argument holds for both Average and Local Directional Displacement Pastes as on a planar base the directional derivatives, along which the \vec{s}_i components are applied, are the same at every point on the surface.

Relative Displacement Paste: Under a linear paste, if the feature boundary Greville displacements and control points were to be mapped into the base domain, they would coincide with the paste curve control points, as seen for a Control Point Paste. If the Greville displacement relationship is maintained by the pasted feature boundary, linear reproduction is expected to hold. An Average Relative Displacement Paste determines the displacement out vector along the barycentre of pasted Greville points to the corresponding pasted Greville point (also a trim point). The barycentre used is identical to the base surface point associated with the paste curve centre used in the base domain displacement construction: $B(\frac{\sum(t_i)}{N-3}) = \frac{\sum B(t_i)}{N-3}$. The out and tangent direction displacements are therefore the same as would be obtained

by mapping the feature through the base domain; this also means that the pasted boundary control points and trim curve control points match up. In the case of a Local Relative Displacement Paste, the linear reproducibility is not as clear. The displacement out vector on the base is determined locally, and even on a planar base it will only be in the direction along the trim curve centre to trim point when the pasted Greville points are equi-spaced. In general, this means that Local Relative Displacement is not necessarily expected to satisfy linearity, whereas Average Relative Displacement should do so.

My actual method implementations do not require identical cylinder boundary and paste curve representations as have been assumed in my linear reproduction assessments above. Identical representations place limitations on the flexibility of trim curve control, and create a dependency of paste improvement upon paste curve refinement. My alternative selection of a simple circular paste curve allows for a more generic performance evaluation of each method. Consequently, however, my approach will reduce C^0 discontinuities with slightly worse than the expected $O(h^2)$ convergence upon progressive cylinder refinement.

Chapter 4

Results

This chapter discusses the results of pasting surfaces using each of the cylindrical pasting techniques developed in this thesis – Greville, Control Point, Directional Displacement, and Relative Displacement pastes. For each method, I present numerical as well as visual paste data to facilitate in quality comparisons of the pasted boundaries and their relative improvements upon knot insertion.

In particular, the empirical error between the pasted feature boundary and the trim curve offers an important comparison metric for evaluation of the feature-on-base boundary quality. The error analysis presented provides a maximum position difference between the two curves as well as a progressive refinement ratio of these differences describing the rate of error convergence.

I evaluate the results of applying each cylindrical pasting scheme to a simple cylinder when pasting onto three different base surfaces of increasing complexity – a planar base, a simple curved base, and a base with an inflection. All the surfaces used were bicubic since bicubic surfaces are most common in computer modelling and animation. As described in the previous section, each paste places the L_0 boundary of a cylindrical feature onto a tensor product base patch, over a join described by a base domain paste curve. For my testing I primarily use circular paste curves, therefore, the feature experimented with was also chosen to have a close-to-circular L_0 boundary. If desired, the pasting methods presented can easily be adapted to non-circular paste curves

(Appendix A). Further, the feature cylinder was constructed with its defining control points describing each u -layer in the counter-clockwise direction as viewed from above. Correspondingly, the paste points within the base domain were also selected counter-clockwise, starting at the zero angle position on the paste circle, in a manner that maintains the relative placement ratios between control points. Alignment during a paste places the first cylinder boundary control point at the zero paste location, and all other positionings follow.

C^0 continuity sampling information was generated by sampling the pasted feature boundary at 10 different positions for each non-overlapping domain interval in the v -parametric direction. These points are compared against samples on the base trim curve given by points associated with the same v -parameter values in the cylinder domain. With each level of feature refinement, the number of samples taken doubles.

For each test case studied, relevant pre-paste data and corresponding pasting results are given in tabular format. The associated snapshots visually demonstrate zero refinement pastes for the same data sets. The control points listed describe the curve or surface with respect to the associated surface's model space. End knots are omitted in the knot vectors, and the trim region is defined by the centre and radius of a paste circle in the base domain.

Figure 4.1 and Table 4.1 show the results of pasting the boundary curve of a bicubic cylinder onto a planar bicubic base patch. As expected, the pasted boundary is identical for all methods except Greville Paste. Although a zero linear error is theoretically expected for all but Greville Paste, the non-zero error arises due to different paste curve and feature boundary representations chosen for control flexibility, as described in §3.8. In these cases, the numerical errors computed offer an estimate of the resulting loss in accuracy. To assert the linear reproducibility and accuracy of my methods, I have included Table 4.2 which performs the same planar paste over a paste curve having representation identical to the feature boundary. As expected, the errors are now seen to be close to zero. The small deviations result both due to floating point computation inaccuracies as well as due to representation differences between the cylinder boundary and paste curve after refinement.

Figure 4.2 and Table 4.3 give the results of pasting the boundary of the same feature cylinder

Base Patch:

knot vector:

u: {0.000, 1.000, 2.000, 3.000, 4.000, 5.000}

v: {0.000, 1.000, 2.000, 3.000, 4.000, 5.000}

control points:

(-3.0, -3.0, 0.0) (-3.0, -1.0, 0.0) (-3.0, 1.0, 0.0) (-3.0, 3.0, 0.0),

(-1.0, -3.0, 0.0) (-1.0, -1.0, 0.0) (-1.0, 1.0, 0.0) (-1.0, 3.0, 0.0),

(1.0, -3.0, 0.0) (1.0, -1.0, 0.0) (1.0, 1.0, 0.0) (1.0, 3.0, 0.0),

(3.0, -3.0, 0.0) (3.0, -1.0, 0.0) (3.0, 1.0, 0.0) (3.0, 3.0, 0.0)

Trim Curve relative base domain:

centre: (2.328, 2.540)

radius: 0.144

Feature Cylinder L_0 :

v-knots: {0.000, 1.000, 2.000, 3.000, 4.000, 5.000, 6.000, 7.000, 8.000, 9.000, 10.000}

control points:

(2.000, 0.000, 0.000), (1.000, 1.732, 0.000), (-1.000, 1.732, 0.000),

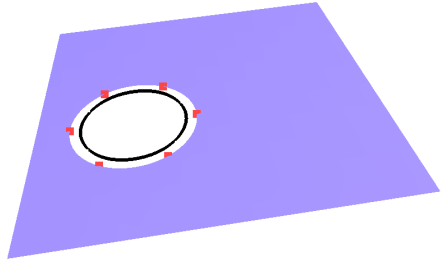
(-2.000, 0.000, 0.000), (-1.000, -1.732, 0.000), (1.000, -1.732, 0.000),

(2.000, 0.000, 0.000), (1.000, 1.732, 0.000), (-1.000, 1.732, 0.000)

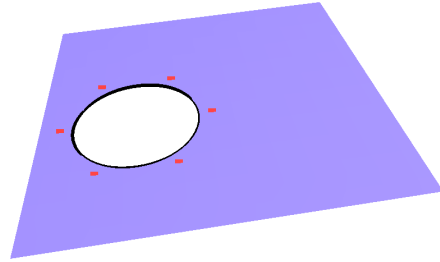
Refinement	Greville		Control Point		Local Directional \vec{d}	
	Max	Ratio	Max	Ratio	Max	Ratio
0	0.048868	na	0.001171	na	0.001171	na
1	0.012891	3.79	0.000365	3.21	0.000365	3.21
2	0.003268	3.94	0.000125	2.91	0.000125	2.91
3	0.000820	3.98	0.000017	7.27	0.000017	7.27
4	0.000205	3.99	0.000002	10.10	0.000002	10.10
5	0.000052	3.98	0.000000	4.44	0.000000	4.44

Refinement	Average Directional \vec{d}		Local Relative \vec{d}		Average Relative \vec{d}	
	Max	Ratio	Max	Ratio	Max	Ratio
0	0.001171	na	0.001171	na	0.001171	na
1	0.000365	3.21	0.000365	3.21	0.000365	3.21
2	0.000125	2.91	0.000125	2.91	0.000125	2.91
3	0.000017	7.27	0.000017	7.27	0.000017	7.27
4	0.000002	10.10	0.000002	10.10	0.000002	10.10
5	0.000000	4.44	0.000000	4.44	0.000000	4.44

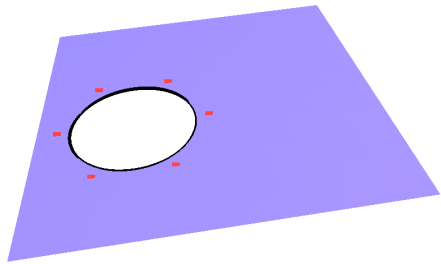
Table 4.1: Experimental Errors – Pasting onto Circular Paste Curve on a Planar Base



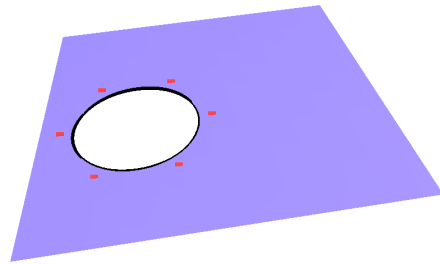
(a) Greville Paste



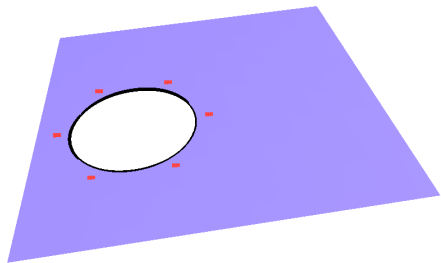
(b) Control Point Paste



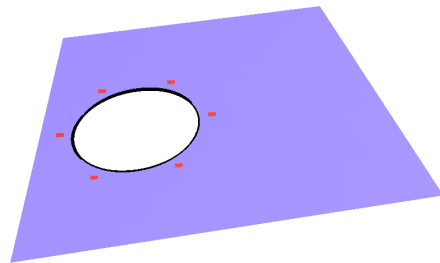
(c) Local Directional \vec{d} Paste



(d) Average Directional \vec{d} Paste



(e) Local Relative \vec{d} Paste



(f) Average Relative \vec{d} Paste

Figure 4.1: Pasting onto a Planar Base

Trim Curve relative base domain:

knots: {0.000, 1.000, 2.000, 3.000, 4.000, 5.000, 6.000, 7.000, 8.000, 9.000, 10.000}

control points:

(2.500, 2.619), (2.440, 2.722), (2.321, 2.722), (2.262, 2.619), (2.321, 2.516),
 (2.440, 2.516), (2.500, 2.619), (2.440, 2.722), (2.321, 2.722)

Refinement	Greville		Control Point		Local Directional \vec{d}	
	Max	Ratio	Max	Ratio	Max	Ratio
0	0.033069	na	0.000001	na	0.000001	na
1	0.009094	3.64	0.000019	0.04	0.000019	0.04
2	0.002377	3.83	0.000018	1.06	0.000018	1.06
3	0.000607	3.91	0.000008	2.19	0.000008	2.19
4	0.000153	3.96	0.000002	4.16	0.000002	4.16
5	0.000039	3.98	0.000000	4.31	0.000000	4.31

Refinement	Average Directional \vec{d}		Local Relative \vec{d}		Average Relative \vec{d}	
	Max	Ratio	Max	Ratio	Max	Ratio
0	0.000001	na	0.000001	na	0.000001	na
1	0.000019	0.04	0.000000	9.67	0.000000	9.67
2	0.000018	1.06	0.000044	0.00	0.000018	0.00
3	0.000008	2.19	0.000020	2.23	0.000008	2.23
4	0.000002	4.16	0.000005	4.21	0.000002	4.20
5	0.000000	4.31	0.000001	4.34	0.000000	4.34

Table 4.2: Experimental Errors – Pasting onto a Polynomial Paste Curve onto the Planar Base of Table 4.1; initial paste curve representation is identical to that of the feature boundary

onto a convex-only curved bicubic base. For this test case it was ensured that the base surface did not have any regions of negative Gaussian curvature. The results demonstrate that Average Directional Displacement Paste and both Relative Displacement Paste methods perform a magnitude better than Greville Paste when pasting onto a convex base. Further, the results support the quadratic error convergence of all the methods.

The final test case pastes the boundary of the same feature cylinder onto a curved bicubic base in a region of negative Gaussian curvature. Pasting is performed for two different trim curves, each containing the region of negative Gaussian curvature, but in different locations. The results are given in Table 4.4 (Figure 4.3) and Table 4.5 respectively. The Relative Displacement Paste methods appear to perform an order of magnitude better when the feature knot structure is approximately as coarse as that of the base. However, even one level of cylinder refinement improves Greville Paste to a level comparable to that achieved by the Relative Displacement techniques. In fact, the minor error reductions offered by the alternatives to Greville Paste are clearly offset by their extra computational costs. This suggests that as the complexity of the base surface increases, the C^0 pasting results obtained using Greville Paste are comparable to all my other simple cylindrical pasting approaches.

Base Patch:

knot vector:

u: {0.000, 1.000, 2.000, 3.000, 4.000, 5.000}

v: {0.000, 1.000, 2.000, 3.000, 4.000, 5.000}

control points:

(-3.0, -3.0, -3.0) (-3.0, -1.0, -3.0) (-3.0, 1.0, -3.0) (-3.0, 3.0, -3.0),
 (-1.0, -3.0, -3.0) (-1.0, -1.0, 3.0) (-1.0, 1.0, 3.0) (-1.0, 3.0, -3.0),
 (1.0, -3.0, -3.0) (1.0, -1.0, 3.0) (1.0, 1.0, 3.0) (1.0, 3.0, -3.0),
 (3.0, -3.0, -3.0) (3.0, -1.0, -3.0) (3.0, 1.0, -3.0) (3.0, 3.0, -3.0)

Trim Curve relative base domain:

centre: (2.381, 2.619)

radius: 0.119

Feature Cylinder L_0 :

v-knots: {0.000, 1.000, 2.000, 3.000, 4.000, 5.000, 6.000, 7.000, 8.000, 9.000, 10.000}

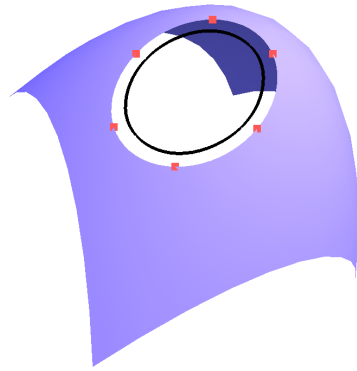
control points:

(2.000, 0.000, 0.000), (1.000, 1.732, 0.000), (-1.000, 1.732, 0.000),
 (-2.000, 0.000, 0.000), (-1.000, -1.732, 0.000), (1.000, -1.732, 0.000),
 (2.000, 0.000, 0.000), (1.000, 1.732, 0.000), (-1.000, 1.732, 0.000),

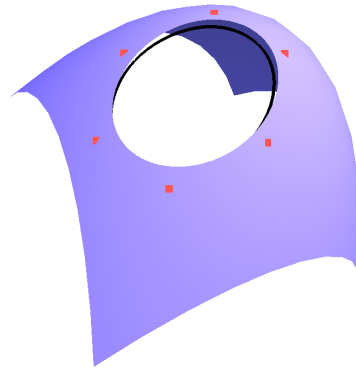
Refinement	Greville		Control Point		Local Directional \vec{d}	
	Max	Ratio	Max	Ratio	Max	Ratio
0	0.044802	na	0.018398	na	0.016778	na
1	0.011866	3.78	0.004594	4.00	0.004500	3.73
2	0.003005	3.95	0.001186	3.87	0.001180	3.81
3	0.000755	3.98	0.000280	4.24	0.000279	4.23
4	0.000189	3.99	0.000067	4.15	0.000067	4.15
5	0.000047	3.98	0.000017	4.00	0.000017	4.00

Refinement	Average Directional \vec{d}		Local Relative \vec{d}		Average Relative \vec{d}	
	Max	Ratio	Max	Ratio	Max	Ratio
0	0.001132	na	0.002182	na	0.002189	na
1	0.001201	0.94	0.001216	1.79	0.001208	1.81
2	0.000369	3.25	0.000396	3.07	0.000394	3.07
3	0.000073	5.05	0.000079	5.03	0.000077	5.14
4	0.000019	3.78	0.000019	4.06	0.000019	3.98
5	0.000005	3.89	0.000005	3.89	0.000005	3.89

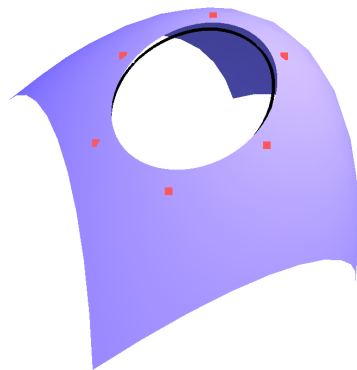
Table 4.3: Experimental Errors – Pasting onto a Convex Base



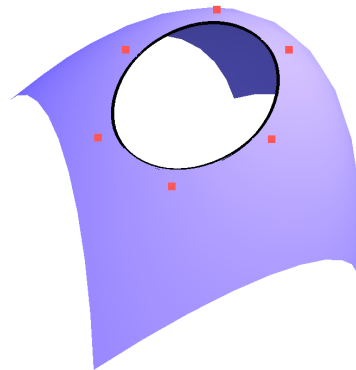
(a) Greville Paste



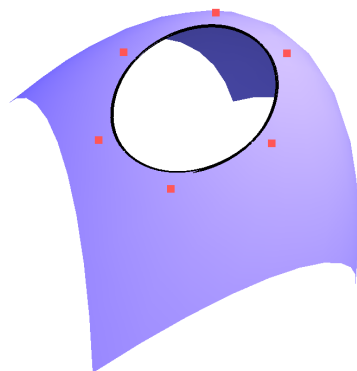
(b) Control Point Paste



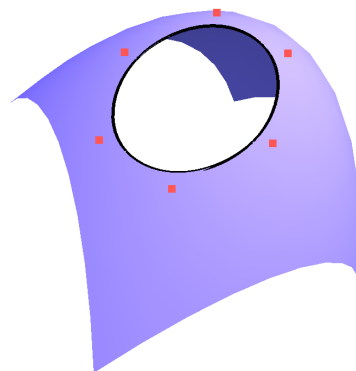
(c) Local Directional \vec{d} Paste



(d) Average Directional \vec{d} Paste



(e) Local Relative \vec{d} Paste



(f) Average Relative \vec{d} Paste

Figure 4.2: Pasting onto a Convex Base

Base Patch:

knot vector:

u: {0.000, 0.000, 0.000, 1.000, 1.000, 1.000, 2.000, 2.000, 2.000}

v: {0.000, 0.000, 0.000, 2.000, 2.000, 2.000}

control points:

(-3.0, 0.0, 2.0) (-3.0, 0.0, 0.0) (-3.0, 0.0, -2.0) (-3.0, 0.0, -4.0),
 (-2.0, 2.0, 2.0) (-2.0, 2.0, 0.0) (-2.0, 2.0, -2.0) (-2.0, 2.0, -4.0),
 (-1.0, 3.0, 2.0) (-1.0, 3.0, 0.0) (-1.0, 3.0, -2.0) (-1.0, 3.0, -4.0),
 (0.0, 2.0, 2.0) (0.0, 2.0, 0.0) (0.0, 2.0, -2.0) (0.0, 2.0, -4.0),
 (1.0, 1.0, 2.0) (1.0, 1.0, 0.0) (1.0, 1.0, -2.0) (1.0, 1.0, -4.0),
 (2.0, -1.0, 2.0) (2.0, -1.0, 0.0) (2.0, -1.0, -2.0) (2.0, -1.0, -4.0),
 (3.0, 1.0, 2.0) (3.0, 1.0, 0.0) (3.0, 1.0, -2.0) (3.0, 1.0, -4.0)

Trim Curve relative base domain:

centre: (1.381, 1.238)

radius: 0.238

Feature Cylinder L_0 :

v-knots: {0.000, 1.000, 2.000, 3.000, 4.000, 5.000, 6.000, 7.000, 8.000, 9.000, 10.000}

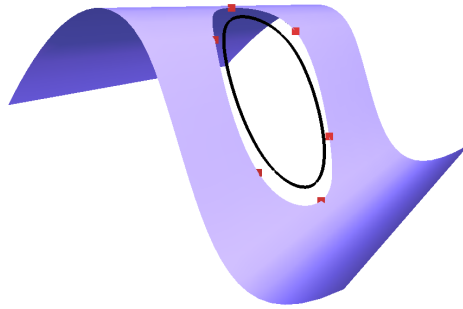
control points:

(2.000, 0.000, 0.000), (1.000, 1.732, 0.000), (-1.000, 1.732, 0.000),
 (-2.000, 0.000, 0.000), (-1.000, -1.732, 0.000), (1.000, -1.732, 0.000),
 (2.000, 0.000, 0.000), (1.000, 1.732, 0.000), (-1.000, 1.732, 0.000)

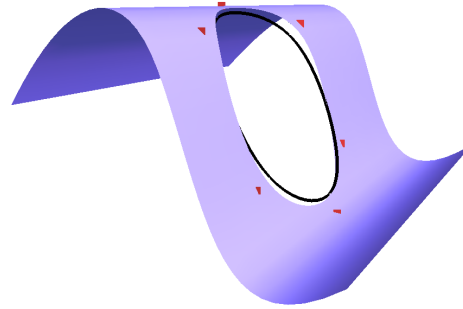
Refinement	Greville		Control Point		Local Directional \vec{d}	
	Max	Ratio	Max	Ratio	Max	Ratio
0	0.185416	na	0.067727	na	0.131738	na
1	0.049609	3.74	0.023591	2.87	0.037600	3.50
2	0.012585	3.94	0.006567	3.59	0.009219	4.08
3	0.003157	3.99	0.001600	4.10	0.002005	4.60
4	0.000790	4.00	0.000359	4.46	0.000473	4.23
5	0.000198	4.00	0.000089	4.05	0.000114	4.15

Refinement	Average Directional \vec{d}		Local Relative \vec{d}		Average Relative \vec{d}	
	Max	Ratio	Max	Ratio	Max	Ratio
0	0.123581	na	0.037246	na	0.039474	na
1	0.035348	3.50	0.014900	2.50	0.018923	2.09
2	0.008783	4.02	0.005125	2.91	0.004766	3.97
3	0.001984	4.43	0.001332	3.85	0.001232	3.87
4	0.000471	4.21	0.000299	4.45	0.000276	4.47
5	0.000113	4.18	0.000073	4.10	0.000067	4.10

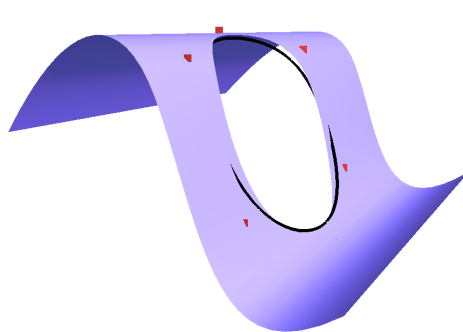
Table 4.4: Experimental Errors – Pasting onto a Convex-Concave Base



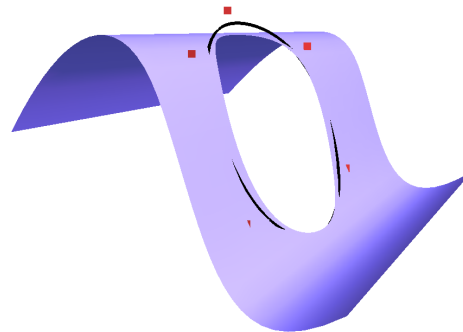
(a) Greville Paste



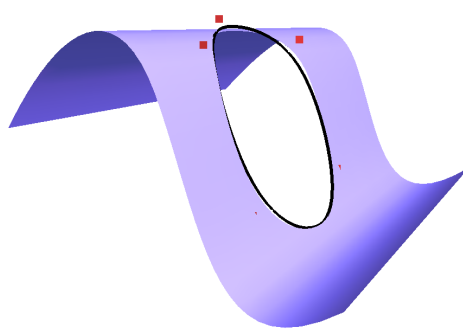
(b) Control Point Paste



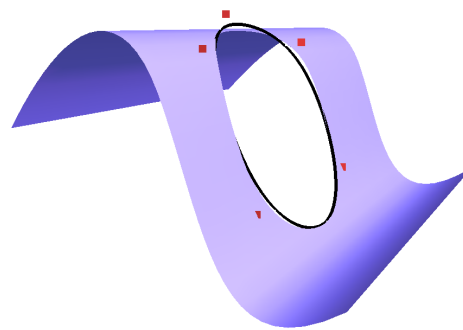
(c) Local Directional \vec{d} Paste



(d) Average Directional \vec{d} Paste



(e) Local Relative \vec{d} Paste



(f) Average Relative \vec{d} Paste

Figure 4.3: Pasting onto a Convex-Concave Base

Base Patch:

knot vector:

u: {0.000, 0.000, 0.000, 1.000, 1.000, 1.000, 2.000, 2.000, 2.000}

v: {0.000, 0.000, 0.000, 2.000, 2.000, 2.000}

control points:

(-3.0, 0.0, 2.0) (-3.0, 0.0, 0.0) (-3.0, 0.0, -2.0) (-3.0, 0.0, -4.0),
 (-2.0, 2.0, 2.0) (-2.0, 2.0, 0.0) (-2.0, 2.0, -2.0) (-2.0, 2.0, -4.0),
 (-1.0, 3.0, 2.0) (-1.0, 3.0, 0.0) (-1.0, 3.0, -2.0) (-1.0, 3.0, -4.0),
 (0.0, 2.0, 2.0) (0.0, 2.0, 0.0) (0.0, 2.0, -2.0) (0.0, 2.0, -4.0),
 (1.0, 1.0, 2.0) (1.0, 1.0, 0.0) (1.0, 1.0, -2.0) (1.0, 1.0, -4.0),
 (2.0, -1.0, 2.0) (2.0, -1.0, 0.0) (2.0, -1.0, -2.0) (2.0, -1.0, -4.0),
 (3.0, 1.0, 2.0) (3.0, 1.0, 0.0) (3.0, 1.0, -2.0) (3.0, 1.0, -4.0)

Trim Curve relative base domain:

centre: (1.190, 1.238)

radius: 0.190

Feature Cylinder L_0 :

v-knots: {0.000, 1.000, 2.000, 3.000, 4.000, 5.000, 6.000, 7.000, 8.000, 9.000, 10.000}

control points:

(2.000, 0.000, 0.000), (1.000, 1.732, 0.000), (-1.000, 1.732, 0.000),
 (-2.000, 0.000, 0.000), (-1.000, -1.732, 0.000), (1.000, -1.732, 0.000),
 (2.000, 0.000, 0.000), (1.000, 1.732, 0.000), (-1.000, 1.732, 0.000)

Refinement	Greville		Control Point		Local Directional \vec{d}	
	Max	Ratio	Max	Ratio	Max	Ratio
0	0.142164	na	0.015252	na	0.092543	na
1	0.037176	3.82	0.014131	1.08	0.025969	3.56
2	0.009377	3.96	0.003657	3.86	0.005259	4.94
3	0.002349	3.99	0.000948	3.86	0.001154	4.56
4	0.000587	4.00	0.000224	4.23	0.000268	4.31
5	0.000147	4.00	0.000054	4.13	0.000063	4.22

Refinement	Average Directional \vec{d}		Local Relative \vec{d}		Average Relative \vec{d}	
	Max	Ratio	Max	Ratio	Max	Ratio
0	0.092532	na	0.012229	na	0.013122	na
1	0.025417	3.64	0.013825	0.88	0.013630	0.96
2	0.005137	4.95	0.004080	3.39	0.004091	3.33
3	0.001150	4.47	0.001022	3.99	0.000962	4.25
4	0.000269	4.27	0.000242	4.23	0.000224	4.29
5	0.000064	4.22	0.000058	4.15	0.000055	4.05

Table 4.5: Experimental Errors – Another Paste onto the Convex-Concave Base of Table 4.4

Chapter 5

Conclusions

5.1 Summary

Surface pasting has come to be recognized as a flexible modelling technique for interactively constructing composite surfaces with regions of local detail. It has even been incorporated into commercially available 3D animation and special effects software packages such as Houdini. The benefits of using surface pasting to construct tensor product patch models encouraged work towards extending the pasting paradigm to include closed-curve blending surfaces. In particular, surface pasting was extended to include tensor product cylinders. However, like patch pasting, cylindrical pasting suffers from a lack of continuity between the pasted feature cylinder and the base. While low-cost alternatives to improve the continuity in patch pasting have been previously explored [4, 9], studies dedicated to efficiently reducing gaps arising at the site of a cylindrical paste have not yet been performed. A fundamental difference between feature cylinders and feature patches suggests that a separate examination is necessary – the closed curve boundary of a cylinder can not be reproduced using zero displacement control points, whereas such a setting, used in standard pasting, works fine for reproducing the linear boundaries of a patch. My work in this thesis was done with the intent of developing an alternative pasting technique appropriate for pasting cylindrical boundaries. To maintain the prototyping nature of pasting, the cylindrical

methods proposed were designed to have low computational costs, i.e., with a paste costing not much more than one base surface evaluation per cylinder boundary control point. Further, hoping to establish a suitable cylindrical pasting standard, all the methods explored were algorithmically simple.

Specifically, I examined six types of control point placements for describing the pasted cylinder boundary – Greville Paste, Control Point Paste, Local Domain Displacement Paste, Average Domain Displacement Paste, Local Relative Displacement Paste, and Average Relative Displacement Paste. Greville Paste is essentially a direct application of standard patch pasting to cylindrical pasting, and its results provide a base metric for evaluation of my methods.

Greville Paste seems intuitively inadequate for pasting cylinders because its placement of pasted control points onto the desired join boundary can never reproduce the corresponding closed curve. Based upon the concepts used to construct the methods, it was expected that Local Domain Displacement Paste would result in the most accurate C^0 paste for any base surface irrespective of its complexity. This expectation was because Local Domain Displacement performs pasting placements using the actual feature control point Greville displacements within the 3D base surface space, accounting for both the shape of the original cylinder boundary as well as the base surface's curvature.

Instead, an empirical analysis of the error between the pasted cylinder boundaries and the desired trim curve indicates that the less-intuitive Relative Displacement Paste methods most consistently produce the best quality join. In the case of a simple convex curved base, a whole order of magnitude improvement is offered over Greville Paste. However, as the complexity of the base surface increases and the pasted boundary is no longer mapped to coplanar points, the relative improvement drops rapidly. It comes as a surprise that, in general, Greville Paste does as well as any of my other cylindrical boundary pasting methods. My results further confirm that the best possible error convergence offered by the methods explored is quadratic in all cases. Therefore, the original standard pasting technique is a reasonable standard not only for patches, but also for cylinders!

5.2 Future Work

This thesis focused on establishing a simple and low-cost cylindrical pasting standard. However, there are still a number of techniques remaining to be assessed in the context of cylindrical pasting. It is recommended that another study be performed to compare the results of cylindrical pasting using methods such as quasi-interpolation, least-squares fitting, and Greville point interpolation. Although the initial computation costs are expected to be notably high for these methods, this may be acceptably and effectively compensated for by low re-evaluation costs when pasting over the same region. An additional concern with these methods can be their algorithmic complexity. For example, applying quasi-interpolation to determine the pasted cylinder's boundary control points will require a number of computational tricks to keep the evaluation costs reasonable. Further, a least-squares fitting will require experimentation with different boundary sampling patterns to see which ones give the best closed curve approximation.

A study of cylindrical pasting cross-boundary derivatives also needs to be performed. Mann and Yeung [12] suggest an alternative to the standard surface pasting technique that appears to reduce the C^1 discontinuity between a base surface and feature cylinder. However, no formal assessment of the error differences has been performed so far. A more exhaustive examination of low-cost ways to improve the C^1 join should simultaneously be considered.

Appendix A

Polynomial Paste Curves

Polynomial paste curves can be used to describe non-circular pasting boundaries within the base domain. If trim curves are later selected directly on the base surface, polynomial paste curves will provide better control as opposed to fitting a circle to the corresponding domain curve. Here I show that all my cylindrical pasting methods can easily be adjusted to work with B-spline paste curves.

The difference is essentially in the determination of the paste points and corresponding 2D displacement frames in the base domain. While circle properties were used for a circular paste curve, B-spline curve evaluations are used for a polynomial paste curve. By generating the B-spline paste curve to have the same curve representation (degree and knot vector) as the unrefined feature cylinder's unpasted boundary, paste points (t_j in Chapter 3) can be obtained as curve points lying at the same Greville abscissae as the cylinder Greville points being associated with them. A vector from the barycentre of paste points to a specific paste point gives the displacement frame out direction, and the tangent is obtained by a curve derivative evaluation. The remaining mappings and computations are the same as described in Chapter 3.

Some experimental tests were run using this alternative paste curve form for data similar to that given in Chapter 4; the results are included as tables in this appendix. As expected, the relative quality of a paste using each cylindrical pasting method was approximately the same

as obtained when pasting onto circular domain curves, confirming that Greville Paste remains a reasonable cylindrical pasting standard.

Base Patch:

knot vector:

u: {0.000, 1.000, 2.000, 3.000, 4.000, 5.000}

v: {0.000, 1.000, 2.000, 3.000, 4.000, 5.000}

control points:

(-3.0, -3.0, -3.0) (-3.0, -1.0, -3.0) (-3.0, 1.0, -3.0) (-3.0, 3.0, -3.0),
 (-1.0, -3.0, -3.0) (-1.0, -1.0, 3.0) (-1.0, 1.0, 3.0) (-1.0, 3.0, -3.0),
 (1.0, -3.0, -3.0) (1.0, -1.0, 3.0) (1.0, 1.0, 3.0) (1.0, 3.0, -3.0),
 (3.0, -3.0, -3.0) (3.0, -1.0, -3.0) (3.0, 1.0, -3.0) (3.0, 3.0, -3.0)

Trim Curve relative base domain:

knots: {0.000, 1.000, 2.000, 3.000, 4.000, 5.000, 6.000, 7.000, 8.000, 9.000, 10.000}

control points:

(2.500, 2.619), (2.440, 2.722), (2.321, 2.722), (2.262, 2.619), (2.321, 2.516),
 (2.440, 2.516), (2.500, 2.619), (2.440, 2.722), (2.321, 2.722)

Feature Cylinder L_0 :

v-knots: {0.000, 1.000, 2.000, 3.000, 4.000, 5.000, 6.000, 7.000, 8.000, 9.000, 10.000}

control points:

(2.000, 0.000, 0.000), (1.000, 1.732, 0.000), (-1.000, 1.732, 0.000),
 (-2.000, 0.000, 0.000), (-1.000, -1.732, 0.000), (1.000, -1.732, 0.000),
 (2.000, 0.000, 0.000), (1.000, 1.732, 0.000), (-1.000, 1.732, 0.000)

Refinement	Greville		Control Point		Local Directional \vec{d}	
	Max	Ratio	Max	Ratio	Max	Ratio
0	0.036708	na	0.012748	na	0.011647	na
1	0.010015	3.67	0.003123	4.08	0.003061	3.80
2	0.002626	3.81	0.000790	3.95	0.000786	3.90
3	0.000672	3.91	0.000199	3.97	0.000199	3.95
4	0.000170	3.95	0.000050	4.02	0.000050	4.01
5	0.000043	3.98	0.000012	4.02	0.000012	4.02

Refinement	Average Directional \vec{d}		Local Relative \vec{d}		Average Relative \vec{d}	
	Max	Ratio	Max	Ratio	Max	Ratio
0	0.000562	na	0.001212	na	0.001219	na
1	0.000949	0.59	0.000918	1.32	0.000922	1.32
2	0.000304	3.12	0.000316	2.90	0.000315	2.93
3	0.000075	4.07	0.000084	3.76	0.000075	4.18
4	0.000018	4.14	0.000021	4.08	0.000018	4.17
5	0.000004	4.05	0.000005	4.08	0.000004	4.06

Table A.1: Experimental Errors – Pasting onto a Polynomial Paste Curve on a Convex Base

Base Patch:

knot vector:

u: {0.000, 0.000, 0.000, 1.000, 1.000, 1.000, 2.000, 2.000, 2.000}

v: {0.000, 0.000, 0.000, 2.000, 2.000, 2.000}

control points:

(-3.0, 0.0, 2.0) (-3.0, 0.0, 0.0) (-3.0, 0.0, -2.0) (-3.0, 0.0, -4.0),
 (-2.0, 2.0, 2.0) (-2.0, 2.0, 0.0) (-2.0, 2.0, -2.0) (-2.0, 2.0, -4.0),
 (-1.0, 3.0, 2.0) (-1.0, 3.0, 0.0) (-1.0, 3.0, -2.0) (-1.0, 3.0, -4.0),
 (0.0, 2.0, 2.0) (0.0, 2.0, 0.0) (0.0, 2.0, -2.0) (0.0, 2.0, -4.0),
 (1.0, 1.0, 2.0) (1.0, 1.0, 0.0) (1.0, 1.0, -2.0) (1.0, 1.0, -4.0),
 (2.0, -1.0, 2.0) (2.0, -1.0, 0.0) (2.0, -1.0, -2.0) (2.0, -1.0, -4.0),
 (3.0, 1.0, 2.0) (3.0, 1.0, 0.0) (3.0, 1.0, -2.0) (3.0, 1.0, -4.0)

Trim Curve relative base domain:

knots: {0.000, 1.000, 2.000, 3.000, 4.000, 5.000, 6.000, 7.000, 8.000, 9.000, 10.000}

control points:

(1.619, 1.238), (1.500, 1.444), (1.262, 1.444), (1.143, 1.238), (1.262, 1.032),
 (1.500, 1.032), (1.619, 1.238), (1.500, 1.444), (1.262, 1.444)

Feature Cylinder L_0 :

v-knots: {0.000, 1.000, 2.000, 3.000, 4.000, 5.000, 6.000, 7.000, 8.000, 9.000, 10.000}

control points:

(2.000, 0.000, 0.000), (1.000, 1.732, 0.000), (-1.000, 1.732, 0.000),
 (-2.000, 0.000, 0.000), (-1.000, -1.732, 0.000), (1.000, -1.732, 0.000),
 (2.000, 0.000, 0.000), (1.000, 1.732, 0.000), (-1.000, 1.732, 0.000)

Refinement	Greville		Control Point		Local Directional \vec{d}	
	Max	Ratio	Max	Ratio	Max	Ratio
0	0.154260	na	0.046186	na	0.107669	na
1	0.042607	3.62	0.013152	3.51	0.022611	4.76
2	0.011133	3.83	0.004414	2.98	0.005415	4.18
3	0.002843	3.92	0.001112	3.97	0.001372	3.95
4	0.000718	3.96	0.000272	4.08	0.000339	4.04
5	0.000181	3.98	0.000067	4.05	0.000085	4.01

Refinement	Average Directional \vec{d}		Local Relative \vec{d}		Average Relative \vec{d}	
	Max	Ratio	Max	Ratio	Max	Ratio
0	0.103268	na	0.029652	na	0.029929	na
1	0.021579	4.79	0.010365	2.86	0.008764	3.41
2	0.005218	4.14	0.003817	2.72	0.003369	2.60
3	0.001357	3.84	0.000939	4.06	0.000865	3.90
4	0.000336	4.04	0.000221	4.25	0.000208	4.15
5	0.000084	4.00	0.000054	4.10	0.000051	4.07

Table A.2: Experimental Errors – Pasting onto a Polynomial Paste Curve on a Convex-Concave Base

Bibliography

- [1] Cristin Barghiel. Feature oriented composition of B-spline surfaces. Master's thesis, University of Waterloo, Waterloo, Ontario, Canada N2L 3G1, 1994. Available as <ftp://cs-archive.uwaterloo.ca/cs-archive/CS-94-13/>.
- [2] Cristin Barghiel, Richard Bartels, and David Forsey. Pasting spline surfaces. In M. Daehlen, T. Lyche, and L. Schumaker, editors, *Mathematical Methods for Curves and Surfaces: Ulvik, Norway*, pages 31–40, Nashville, TN., 1995. Vanderbilt University Press.
- [3] Richard Bartels and David Forsey. Spline overlay surfaces. Technical Report CS-92-08, University of Waterloo, Waterloo, Ontario, Canada N2L 3G1, 1991.
- [4] Blair Conrad. Better pasting through quasi-interpolation. Master's thesis, University of Waterloo, Waterloo, Ontario, Canada N2L 3G1, 1999. Available as <ftp://cs-archive.uwaterloo.ca/cs-archive/CS-99-14/>.
- [5] Blair Conrad and Stephen Mann. Better pasting via quasi-interpolation. In Pierre-Jean Laurent, Paul Sablonnière, and Larry Schumaker, editors, *Curve and Surface Design: Saint-Malo, 1999*, pages 27–36, Nashville, TN., 2000. Vanderbilt University Press.
- [6] Gerald Farin. *Curves and Surfaces for Computer Aided Geometric Design: A Practical Guide*. Academic Press, fourth edition, 1997.
- [7] James Foley, Andries vanDam, Steven Feiner, and John Hughes. *Computer Graphics Principles and Practice*. Addison-Wesley, second edition, 1990.

- [8] David Forsey and Richard Bartels. Hierarchical B-Spline refinement. In *Computer Graphics (SIGGRAPH '88)*, volume 22(4), pages 205–212, August 1988.
- [9] Rick Leung. Distortion minimization and continuity preservation in surface pasting. Master's thesis, University of Waterloo, Waterloo, Ontario, Canada N2L 3G1, 2002.
- [10] Rick Leung and Stephen Mann. Distortion minimization and continuity preservation in surface pasting. In *Graphics Interface*, pages 193–200, May 2003.
- [11] Stephen Mann and Tony DeRose. Computing values and derivatives of Bézier and B-spline tensor products. In *Computer Aided Geometric Design*, volume 12(1), pages 107–110, February 1995.
- [12] Stephen Mann and Teresa Yeung. Cylindrical surface pasting. Technical Report CS-99-13, University of Waterloo, Waterloo, Ontario, Canada N2L 3G1, 1999. Available as <ftp://cs-archive.uwaterloo.ca/cs-archive/CS-99-13/>.
- [13] Stephen Mann and Teresa Yeung. Cylindrical surface pasting. In *Geometric Modelling*, pages 233–248. Springer-Wein, 2001.
- [14] Lyle Ramshaw. Blossoming: A connect-the-dots approach to splines. Technical Report 19, Digital Systems Research Center, Palo Alto, CA, 1987.
- [15] Selina Siu. Computer aided ferret design. Master's thesis, University of Waterloo, Waterloo, Ontario, Canada N2L 3G1, 2003.
- [16] Eric Stollnitz, Tony DeRose, and David Salesin. *Wavelets for Computer Graphics: Theory and Applications*. Morgan Kaufmann, San Francisco, 1996.
- [17] J. Vida, R. R. Martin, and T. Várady. A survey of blending methods that use parametric surfaces. In *Computer Aided Design*, volume 26(5), pages 341–365, 1994.
- [18] David Wells. *The Penguin Dictionary of Curious and Interesting Geometry*. Penguin, 1991.